Research Article
Cirrhosis

JOURNAL
OF HEPATOLOGY

FXR-modulates the gut-vascular barrier by regulating the entry sites for bacterial translocation in experimental cirrhosis

Graphical abstract

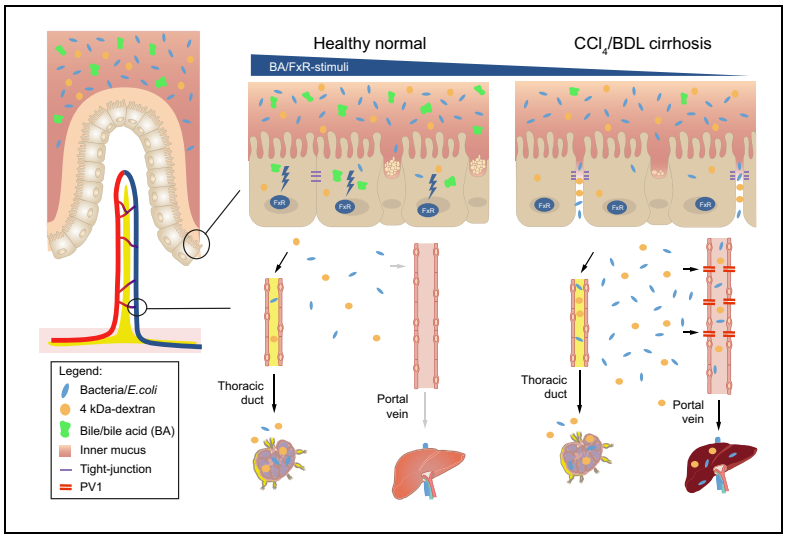

Highlights

- For intestinal bacteria to enter the systemic circulation they must cross the mucus, epithelial and gut-vascular barrier.
- Cirrhosis, but not portal hypertension *per se*, grossly impairs the endothelial and muco-epithelial barriers.
- This promotes pathological bacterial translocation via the portal-venous circulation.
- Both barriers appear to be FXR-modulated, as FXR-agonists reduce portal-venous bacterial translocation.

Authors

Marcel Sorribas, Manuel O. Jakob, Bahtiyar Yilmaz, ..., Ilaria Spadoni, Maria Rescigno, Reiner Wiest

Correspondence

Reiner.wiest@insel.ch
(R. Wiest)

Lay summary

For intestinal bacteria to enter the systemic circulation, they must cross the mucus and epithelial layer, as well as the gut-vascular barrier. Cirrhosis disrupts all 3 of these barriers, giving bacteria access to the portal-venous circulation and thus, the gut-liver axis. Diminished luminal bile acid availability, cirrhosis and the associated reduction in farnesoid x receptor (FXR) signaling seem, at least partly, to mediate these changes, as FXR-agonists reduce bacterial translocation via the portal-venous route to the liver in cirrhosis.

http://dx.doi.org/10.1016/j.jhep.2019.06.017

Research Article
Cirrhosis

JOURNAL OF HEPATOLOGY

FXR-modulates the gut-vascular barrier by regulating the entry sites for bacterial translocation in experimental cirrhosis

Marcel Sorribas[1], Manuel O. Jakob[2], Bahtiyar Yilmaz[1], Hai Li[1], David Stutz[2], Yannik Noser[2], Andrea de Gottardi[2], Sheida Moghadamrad[1], Moushin Hassan[1], Agustin Albillos[3], Ruben Francés[4], Oriol Juanola[4], Ilaria Spadoni[5], Maria Rescigno[5,6], Reiner Wiest[1,2,*]

[1]*Maurice Müller Laboratories, Department for Biomedical Research, University of Bern, Bern, Switzerland;* [2]*Department of Visceral Surgery and Medicine, Bern University Hospital, University of Bern, Bern, Switzerland;* [3]*Department of Gastroenterology, Hospital Universitario Ramón y Cajal, IRYCIS, Madrid, Spain;* [4]*Hepatic and Intestinal Immunobiology Group, Universidad Miguel Hernández-CIBERehd, San Juan, Spain;* [5]*Humanitas University, Department of Biomedical Sciences, Via Rita Levi Montalcini, 20090 Pieve Emanuele, MI, Italy;* [6]*Humanitas Clinical and Research Center, Via Manzoni 56, 20089 Rozzano, MI, Italy*

Background & Aims: Pathological bacterial translocation (PBT) in cirrhosis is the hallmark of spontaneous bacterial infections, increasing mortality several-fold. Increased intestinal permeability is known to contribute to PBT in cirrhosis, although the role of the mucus layer has not been addressed in detail. A clear route of translocation for luminal intestinal bacteria is yet to be defined, but we hypothesize that the recently described gut-vascular barrier (GVB) is impaired in experimental portal hypertension, leading to increased accessibility of the vascular compartment for translocating bacteria.

Materials: Cirrhosis was induced in mouse models using bile-duct ligation (BDL) and CCl_4. Pre-hepatic portal-hypertension was induced by partial portal vein ligation (PPVL). Intestinal permeability was compared in these mice after GFP-*Escherichia coli* or different sized FITC-dextrans were injected into the intestine.

Results: Healthy and pre-hepatic portal-hypertensive (PPVL) mice lack translocation of FITC-dextran and GFP-*E. coli* from the small intestine to the liver, whereas BDL and CCl_4-induced cirrhotic mice demonstrate pathological translocation, which is not altered by prior thoracic-duct ligation. The mucus layer is reduced in thickness, with loss of goblet cells and Muc2-staining and expression in cirrhotic but not PPVL mice. These changes are associated with bacterial overgrowth in the inner mucus layer and pathological translocation of GFP-*E. coli* through the ileal epithelium. GVB is profoundly altered in BDL and CCl_4-mice with Ileal extravasation of large-sized 150 kDa-FITC-dextran, but only slightly altered in PPVL mice. This pathological endothelial permeability and accessibility in cirrhotic mice is associated with augmented expression of PV1 in intestinal vessels. OCA but not fexaramine stabilizes the GVB, whereas both FXR-agonists ameliorate gut to liver translocation of GFP-*E. coli*.

Conclusions: Cirrhosis, but not portal hypertension *per se*, grossly impairs the endothelial and muco-epithelial barriers, promoting PBT to the portal-venous circulation. Both barriers appear to be FXR-modulated, with FXR-agonists reducing PBT via the portal-venous route.

Lay summary: For intestinal bacteria to enter the systemic circulation, they must cross the mucus and epithelial layer, as well as the gut-vascular barrier. Cirrhosis disrupts all 3 of these barriers, giving bacteria access to the portal-venous circulation and thus, the gut-liver axis. Diminished luminal bile acid availability, cirrhosis and the associated reduction in farnesoid x receptor (FXR) signaling seem, at least partly, to mediate these changes, as FXR-agonists reduce bacterial translocation via the portal-venous route to the liver in cirrhosis.

Introduction

The gut-liver axis represents the pathophysiological hallmark for initiation and/or perpetuation of multiple liver diseases[1] and has been proposed to be fueled by pathological bacterial translocation (PBT) from the gut.[2] In liver cirrhosis, PBT from the gut into the liver and systemic circulation is one of the causes of bacterial infections and the augmented pro-inflammatory response to gut-derived products.[2,3] In fact, failure to control invading bacteria and bacterial products in concert with host susceptibility determines remote organ injury in liver cirrhosis. This may include acute-on-chronic liver failure, hepatorenal syndrome and hepatic encephalopathy, which are all associated with worsening prognosis.[4] PBT in liver cirrhosis has been attributed to small intestinal bacterial overgrowth, increased intestinal permeability and lack of host defense mechanisms.[5] Herein, we focused on the first and last barrier separating luminal bacteria and the vascular compartment, namely intestinal mucus and the newly defined gut-vascular barrier (GVB),[6] neither of which have been addressed so far in liver cirrhosis and PBT.

Mucus represents the first frontier that commensal microbes in the gut have to cross in order to achieve PBT. The mucus consists of 2 layers with a similar protein composition where

Keywords: Portal hypertension; Liver cirrhosis; Gut-liver axis; Gut-vascular barrier; Intestinal permeability; Mucus; FXR.
Received 14 December 2018; received in revised form 26 May 2019; accepted 19 June 2019

* Corresponding author. Address: Department Gastroenterology, Inselspital, University Hospital, Bern 3010, Switzerland. Tel.: +41 31 632 0591, Fax: +41 31 632 2988.
E-mail address: Reiner.wiest@insel.ch (R. Wiest).

Please cite this article in press as: Sorribas M et al. FXR-modulates the gut-vascular barrier by regulating the entry sites for bacterial translocation in experimental cirrhosis. J Hepatol (2019), https://doi.org/10.1016/j.jhep.2019.06.017

mucin-2 (MUC2) is the main component.[7] On one hand, the inner mucus layer is firmly attached to the epithelium, is densely packed and is devoid of bacteria.[8] On the other hand, the outer mucus layer is much more mobile, looser and is colonized with a distinct bacterial community.[9] Goblet cells (GCs) are responsible for the formation of both the inner and outer mucus layer[10] but also sense bacteria[11] and react accordingly with mucin secretion.[12,13] After crossing the mucus and epithelial barrier, translocating bacteria reach the lymphatic system, as shown by culture positive mesenteric lymph nodes in experimental cirrhosis in multiple independent studies.[14,15] In contrast, access to the intestinal microcirculation and portal-venous route has been proposed for PBT,[16] but has not been delineated in detail in portal hypertension and liver cirrhosis yet. The splanchnic circulation in portal hypertension presents with multiple vascular abnormalities[17] including arterial vasodilation,[14] hyporesponsiveness to vasoconstrictors[18,19] and increased angiogenesis.[20] However, accessability of the intestinal microcirculation and thus, portal-venous route has not been investigated in portal hypertension so far. Endothelial barriers are characterized by the presence of junctional complexes which strictly control paracellular trafficking of solutes, fluids and cells.[21] In healthy conditions, the endothelial vascular barrier discriminates between differently sized particles of the same nature with 4 kDa-dextran freely diffusing through the endothelium, whereas 70 kDa-dextran does not. Plasmalemma vesicle-associated protein (PV)-1 is an endothelial cell-specific protein that forms the stomatal and fenestral diaphragms of blood vessels[22] and regulates basal permeability.[23]

Liver cirrhosis is characterized by deficient levels of luminal bile acids in the gut.[24] Bile acids have been long known for their major effects on the microbiome and the intestinal barrier function. They exert their effects via transcription factors among which the farnesoid X receptor (FXR) is known to be one of the most important. FXR activation has been reported to influence epithelial cell proliferation[25] and to exert potent anti-inflammatory actions in the intestine, stabilizing epithelial integrity.[26–29] Moreover, FXR stimulation in the small intestine exerts antibacterial actions via induction of antimicrobial substances[30] and FXR-agonists have been shown to ameliorate chemically induced intestinal inflammation, improving symptoms of colitis and inhibiting epithelial permeability. However, the exact role of bile acids and FXR in controlling intestinal muco-epithelial as well as vascular permeability is still unknown. In addition, the microbiome has been proposed to play a key role in mucus synthesis, release and barrier-function[31] but information on its impact on GC density and mucus thickness are limited. Finally, although colonization by microbial commensals is known to promote vascular development[32] its impact and modulatory role on the GVB-function is not known.

Taken together, the aims of the current study were i) to characterize changes in the mucus barrier, as well as GVB, in germ-free conditions and in the context of liver cirrhosis or portal hypertension; ii) to delineate PBT from the gut to the liver along the gut-liver axis in liver cirrhosis; iii) to unravel the role(s) of FXR on PBT, the mucus barrier and GVB.

Materials and methods

Mice and animal models

Female C57BL/6J mice were purchased from ENVIGO (Horst, The Netherlands) and kept at the Central Animal Facility of the University of Bern under specific pathogen-free (SPF) conditions. Mice were kept in next-generation IVC cages with an enriched environment, 12 h day-night cycle and fed *ad libitum*. All experiments involving animals were performed in accordance with Swiss Federal regulations and with local institutional approval. Where indicated, animals were kept in either germ-free conditions or gnotobiotic conditions (with a stable defined moderately diverse mouse microbiota [sDMDM2] that consists of 12 bacterial species) which have been developed and used previously in our lab.[9] The intestine-specific *Fxr*-null ($Fxr^{\Delta IE}$) mice are on a C57BL/6 genetic background and kindly provided by Prof. B. Schnabl from University of California San Diego, USA.

Bile-duct ligation

Bile-duct ligation (BDL) was performed as previously described.[33] Briefly, in an aseptic setting, the abdomen was incised in the midline under isoflurane anesthesia and administration of buprenorphine 60 μg/kg body weight. The bile duct was then cleared from adjacent structures. Three different ligatures were placed along the bile duct with a non-absorbable suture and the bile duct was resected between the second and third ligature. Sham-operated mice were treated similarly but no ligature was placed. Experiments were performed 10 days to 4 weeks after surgery.

Partial portal vein ligation

To induce pre-hepatic portal hypertension, partial portal vein ligation (PPVL) was performed as follows: in an aseptic setting, the abdomen was incised in the midline under isoflurane anesthesia and administration of buprenorphine 60 μg/kg body weight. The portal vein was cleared from surrounding tissue. To achieve only partial and not complete ligation, a non-absorbable suture was placed around a 26-gauge blunt-tipped needle lying alongside the portal vein. After ligation the blunt-tipped needle was removed, leaving a calibrated stenosis on the portal vein. Sham-operated mice were treated the same with no ligature placed. Experiments were performed 14 days after surgery.

CCl_4-induced cirrhosis

Cirrhosis was induced according to the method described before in rats (Runyon, Sugano, Kanel, & Mellencamp, 1991) and modified for mice.[34] After 1 week of phenobarbital administration in the drinking water (0.3 g/L), CCl_4 inhalation was started: mice were placed 3 times per week in a gas chamber and compressed air, bubbling through a flask containing CCl_4, was passed into the gas chamber via a flowmeter (2 L/min). Afterwards, bubbling was stopped and animals were left to breath normal air. The length of CCl_4 exposure was progressively increased, 1 min of bubbling the first week, 1.5 min of bubbling in the second week, and then 2 min of bubbling throughout the rest of the experiment. Mice were treated with 1 cycle/treatment in the initial 3 weeks, with 2 cycles/treatment in the fourth week, and with 3 cycles/treatment thereafter. Once treatment consisted of 2 or more cycles, these were separated by at least 10 min of breathing in ambient air not containing CCl_4.

Thoracic-duct ligation

Thoracic-duct ligation was performed as previously described with some alterations.[35] After gavage of an oil solution 30 min prior to the operation, mice were anesthetized and a left-sided subcostal incision was performed. After incision of the dorsal

Please cite this article in press as: Sorribas M et al. FXR-modulates the gut-vascular barrier by regulating the entry sites for bacterial translocation in experimental cirrhosis. J Hepatol (2019), https://doi.org/10.1016/j.jhep.2019.06.017

retroperitoneum, the aorta was freed from surrounding fatty tissue. The thoracic duct was exposed and carefully freed from the aorta. A metal clip was then placed for closure of the thoracic duct (Clip 9 Vitalitec, Peters Surgical, Bobigny Cedex, France). The incision was closed with a 2-layer running suture (Prolene 6-0, Ethicon, Johnson & Johnson, Spreitenbach, Switzerland).

Pharmacologic FXR modulation

Pharmacological FXR modulation was achieved by high-affinity FXR-agonists, namely fexaramine (Fex)[36] and obeticholic acid (OCA)[37] treatment by oral gavage. Fex is known to lack major absorption and systemic appearance (<30 nm per oral 100 mg/kg/day). Thus, its activity is focused luminally in the intestine, and hence at the muco-epithelial site.[38] In contrast, OCA *per os* is rapidly and highly absorbed, achieving sufficient systemic drug levels (>10 μmol in serum after 30 mg/kg/day[39]), thus targeting the muco-epithelial, endothelial and hence, GVB.

***In vivo* permeability and intestinal loop assay**

Mice were placed under isoflurane anesthesia; middle line laparotomy was performed and the terminal ileum was exteriorized and 1 cm of terminal ileum ligated. A total of 8 mg of 4 kDA FITC-dextran (Sigma-Aldrich) or GFP-*E. coli* (10^5 colony-forming units [CFUs]) were injected in the loop dissolved in 200 μl of saline. One hour after injecting the liver, mesenteric lymph nodes (MLNs), spleen and the intestinal loop were harvested and fixed in Carnoy's fixative (60% Ethanol, 30% Chloroform, 10% glacial acetic acid) and embedded in paraffin. The amount of the dye was measured in the liver, spleen and MLN by immunofluorescence of 5 μm sections stained with 4′,6-diamidin-2-fenilindolo (DAPI). Number of particles (FITC-signal or GFP-*E. coli*) were counted per high-power field at 40x in a fluorescence microscope (Nikon, Eclipse Ti-E). In some experiments, prior to isolation of the loop and inoculation of FITC-dextran or GFP-*E. coli* the thoracic duct was ligated to avoid any lymphatic drainage of translocating agents into the systemic circulation that otherwise could contribute to the hepatic counts. To control for tissue auto-fluorescence some intestinal loops were injected with saline and no particles were counted in the tissue harvested from these mice.

***In vivo* intravital probe-based confocal laser endomicroscopy**

Mice were placed under isoflurane anesthesia and 1 cm long incision was made on the skin to expose the peritoneal wall. An additional small incision was made on the peritoneum to expose the abdominal cavity. A 3 cm to 4 cm loop from the ileum was externalized and endomicroscopy probe (ColoFlex™ UHD, Mauna Kea Technologies) was fixed at an angle of 60° from the operation table close to the exposed intestinal loop. A small incision was made in the anti-mesenteric surface of the intestinal wall and the endomicroscopy probe was inserted in the intestine. The probe was placed so that at least 1 villus was visualized on the screen. After stable imaging was achieved a retro-orbital intravenous injection was made with a FITC-dextran solution (50 μl of 40 mg/ml for 4 kDa-FITC-dextran, 50 μl of 10 mg/ml for 40 kDa and 70 kDa-FITC-dextran or 100 μl of 10 mg/ml for 150 kDa-FITC-dextran solution from SIGMA). Immediately after the injection, the FITC signal was observed in the intestinal villi capillaries and the intestine was pulled using forceps in order to scan the epithelial surface. An endoscopy video was recorded for 30 min of total observation time.

Endothelial leakage analysis from *in vivo* endomicroscopy

Cellvizio Viewer software (Mauna Kea Technologies) was used in order to extract the photograms from the endomicroscopy video. The images with focused vessels and normal blood flow were selected. At least 1 picture per time point was selected and 7 measurements were taken per picture. Measurements were made using Image J as follows: straight lines perpendicular to the vessel were drawn in each vessel within the picture and grey value measured in each pixel along the line. Mean grey value (MGV) of the vessel was calculated and background fluorescence was extracted, MGV of the immediate extravascular space was calculated in the same way. To avoid a bias in our measurements we took the same numbers of pixels analyzed from the intra and extravascular space in all the mice. We also avoid measuring these extravascular spaces where more than 1 vessel could contribute to the fluorescence values. Results are shown as a ratio between mean of extravascular fluorescence and mean of intravascular fluorescence. When extravasation was too high to distinguish vessels from lamina propria a value of 1 was given arbitrarily.

Interepithelial leakage analysis from *in vivo* endomicroscopy

Cellvizio Viewer software (Mauna Kea Technologies) was used in order to extract the photograms from the endomicroscopy video. Only these photograms where the vessels were in focus and properly perfused were selected. The first time when the majority of the interepithelial spaces were seen positive for fluorescein was noted. When this requirement was not accomplished a value of 30 min was given.

Dual-band confocal laser endomicroscopy *in vivo* in intestinal loop experiments

Mice were anesthetized with an isofluorane-oxygen mixture. Laparotomy was performed and terminal ileum intestinal loop exposed. Endomicroscopy probe (UltraMiniO) was fixed at an angle of 60° from the operating table close to the exposed intestinal loop. A small incision was made in the anti-mesenteric surface of the intestinal wall and the endomicroscopy probe was inserted in the intestine. The probe was placed so that at least 1 villus was visualized on the screen. After stable imaging was achieved, 1 ligature was placed 1 cm proximal to the gut opening and another around the probe and the gut itself. After ligation retro-orbital intravenous injection of 100 μl of 2% Evans blue (SIGMA) solution was performed. GFP-*E. coli* was injected to the loop (10^5 CFU in 0.2 ml media). Visualization of *E.coli* and intestinal villi capillaries was performed using Cellvizio ® Dual Band (Mauna Kea Technologies) for 1 h.

Immunofluorescence and confocal microscopy for endothelial cell-to-cell-interactions and PV-1

Intestinal samples were fixed overnight in paraformaldehyde, L-Lysine pH 7.4 and NaIO4 (PLP buffer). They were then washed, dehydrated in 20% sucrose overnight and included in the optimal cutting temperature compound. Cryosections of 10 μm were rehydrated, blocked with 0.1 M Tris-HCl pH 7.4, 2% FBS, 0.3% Triton X-100 and stained with the following antibodies: anti-mouse PV-1 or PLVAP (clone MECA32, BD Pharmingen), anti-ZO1 (clone ZO1-1A12, Invitrogen), anti-Occludin (clone OC-3F10, Invitrogen), anti-mouse CD34 (clone RAM34, eBioscience). Slices were then incubated with the appropriate fluorophore-conjugated secondary antibody. Before imaging, nuclei were counterstained with DAPI. Confocal microscopy

Please cite this article in press as: Sorribas M et al. FXR-modulates the gut-vascular barrier by regulating the entry sites for bacterial translocation in experimental cirrhosis. J Hepatol (2019), https://doi.org/10.1016/j.jhep.2019.06.017

was performed on a Leica TCS SP5 laser confocal scanner mounted on a Leica DMI 6000B inverted microscope equipped with motorized stage. Image J software package was used for image analysis and fluorescence quantification.

Goblet cell analysis

Sections (1 cm) of different parts of the small intestine (duodenum, jejunum and ileum) and colon were fixed in Carnoy's fixative (60% Methanol, 30% Chloroform and 10% Glacial acetic acid) overnight and embedded in paraffin. Thin cuts of 6 μm were deparaffinized and GC stained with periodic acid-Schiff solution (PAS) and hematoxylin to stain nuclei. Pictures were taken at 200x magnification with a bright field microscope GC were counted and villi perimeter measured using Image J. We have demonstrated that perimeter of the villi strongly correlates ($R^2 = 0.9028$) with the number of epithelial cells (data not shown). Hence the ratio between the number of GCs and perimeter is representative of the proportion of GCs amongst epithelial cells in a given villus.

Mucus parameters

Mucus thickness measurements in gut explants were performed using a micromanipulator holding a cell injection pipette with the corresponding glass capillary tilted to a delivered angle. The position of the capillary was recorded when touching the mucus layer and recorded again when touching the villus, visualized under a stereomicroscope. Mucus thickness was calculated via trigonometrical approach as the product between the measured distance and the sinus of the given angle. Five measurements per organ were performed. The inner mucus layer in sDMDM2-conditions was assessed for bacterial load after removing the outer layer by suction, harvesting manually and culturing on lysogeny broth agar plates for 12 h. Results were shown as CFUs per mg mucus.

Electron microscopy

Mouse intestine was fixed with 2.5% glutaraldehyde (Agar Scientific, Stansted, Essex, UK) and 2% paraformaldehyde (Merck, Darmstadt, Germany) in 0.1 M Na-cacodylate-buffer (Merck, Darmstadt, Germany) with a pH of 7.33. Samples were fixed for at least 24 h before being further processed. Samples were then washed with 0.1 M Na-cacodylate-buffer 3 times, each for 5 min, post-fixed with 1% OsO4 (Electron Microscopy Sciences, Hatfield, USA) in 0.1 M Na-cacodylate-buffer at 4 °C for 2 h, and then washed in 0.05 M maleic acid (Merck, Darmstadt, Germany) 3 times, each for 5 min. Thereafter samples were dehydrated in 70, 80, and 96% ethanol (Alcosuisse, Switzerland) for 15 min each at room temperature. Subsequently, the tissue was immersed in 100% ethanol (Merck, Darmstadt, Germany) 3 times, each for 10 min, in acetone (Merck, Darmstadt, Germany) 2 times, each for 10 min, and finally in acetone-Epon (1:1) overnight at room temperature. The next day, samples were embedded in Epon (Sigma-Aldrich, Buchs, Switzerland) and left to harden at 60 °C for 5 days. Sections were produced with an ultramicrotome UC6 (Leica Microsystems, Vienna, Austria), first semithin sections (1 μm) for light microscopy, which were stained with a solution of 0.5% toluidine blue O (Merck, Darmstadt, Germany), and then ultrathin sections (75 nm) for electron microscopy. The sections, mounted on 200 mesh copper grids, were stained with uranyless (Electron Microscopy Sciences, Hatfield, USA) and lead citrate (Leica Microsystems, Vienna, Austria) with an ultrostainer (Leica Microsystems, Vienna, Austria). Sections were then examined with a transmission electron microscope (CM12, Philips, Eindhoven) equipped with a digital camera (Morada, Soft Imaging System, Münster, Germany) and image analysis software (iTEM).

RNA sequencing and network analysis

Whole tissue RNA was extracted from frozen ileum sections by homogenizing with Tissue Lyzer (QIAGEN) and TRIzol reagent (Life Technologies). A total of 200 μl of chloroform was added, samples mixed and centrifuged for 10 min. The upper RNA-containing phase was recovered and RNA precipitated with ice-cold isopropanol. The solution was centrifuged and the RNA pellet washed with 75% ethanol. Once dried, it was resuspended in RNase-free water. Concentration and purity was measured with Bioanalyzer (AGILENT). Library preparation was done using the RIboMinus protocol. Libraries were sequenced by Illumina HiSeq 3000 on the 100 bp paired-end mode. The quality of the reads was documented as well as the number of them and they were mapped to the mouse genome. The number of reads per gene was compared to the different experimental groups using DESeq2 package from R software. Adjusted *p* value and log2 fold-change was calculated according to Benjamini and Hochberg, 1995. Protein-protein interactions were performed using the STRIG database for these proteins whose genes were significantly upregulated (log2 fold-change higher than 2 and adjusted *p* value lower than 0.01).

Statistical analysis

Statistical differences were evaluated using GraphPad Prism software Version7.0. The values were compared using either Student's *t* test or ANOVA. Survival analysis were performed by Mantel-Cox-analysis. In all the cases, the statistical test used is indicated in each figure legends. Results were represented as mean ± SEM. $^{*}p$ <0.05, $^{**}p$ <0.01, $^{***}p$ <0.001.

Results

Increased gut-liver translocation in intestinal loop experiments in cirrhotic but not pre-hepatic portal-hypertensive mice

In control mice, as well as in PPVL-animals, neither GFP-*E. coli* nor 4 kDa-FITC-dextran translocated from the ileum to the liver (Fig. 1A). However, 4 kDa-FITC-dextran, as well as GFP-*E. coli,* were detectable in high numbers and hence, significantly increased in translocation to the liver in cirrhotic (BDL and CCl_4-treated) mice (Fig. 1B). This was also confirmed *in vivo* by applying the dual-band laserendomicroscopy to the liver 1 h after loading the intestinal loop with GFP-*E. coli* (Fig. S1). In animals with prior ligation of the thoracic duct, the number of GFP-*E. coli* observed intrahepatically was not significantly altered (Fig. 1C), suggesting that penetrating intestinal bacteria reach the liver mainly via the portal-venous circulation within the protocol applied here.

Lymphatic route of bacterial translocation is physiologically active and increased in intestinal loop experiments in BDL cirrhotic but not in pre-hepatic portal-hypertensive mice

In healthy mice, 4 kDa-FITC-dextran (not shown) as well as GFP-*E. coli* translocated from ileal loop to MLNs and Peyer's patches (PPs), demonstrating a physiological low rate of translocation along the lymphatic route (Fig. S2A). This lymphatic bacterial translocation was not increased in PPVL mice but

Please cite this article in press as: Sorribas M et al. FXR-modulates the gut-vascular barrier by regulating the entry sites for bacterial translocation in experimental cirrhosis. J Hepatol (2019), https://doi.org/10.1016/j.jhep.2019.06.017

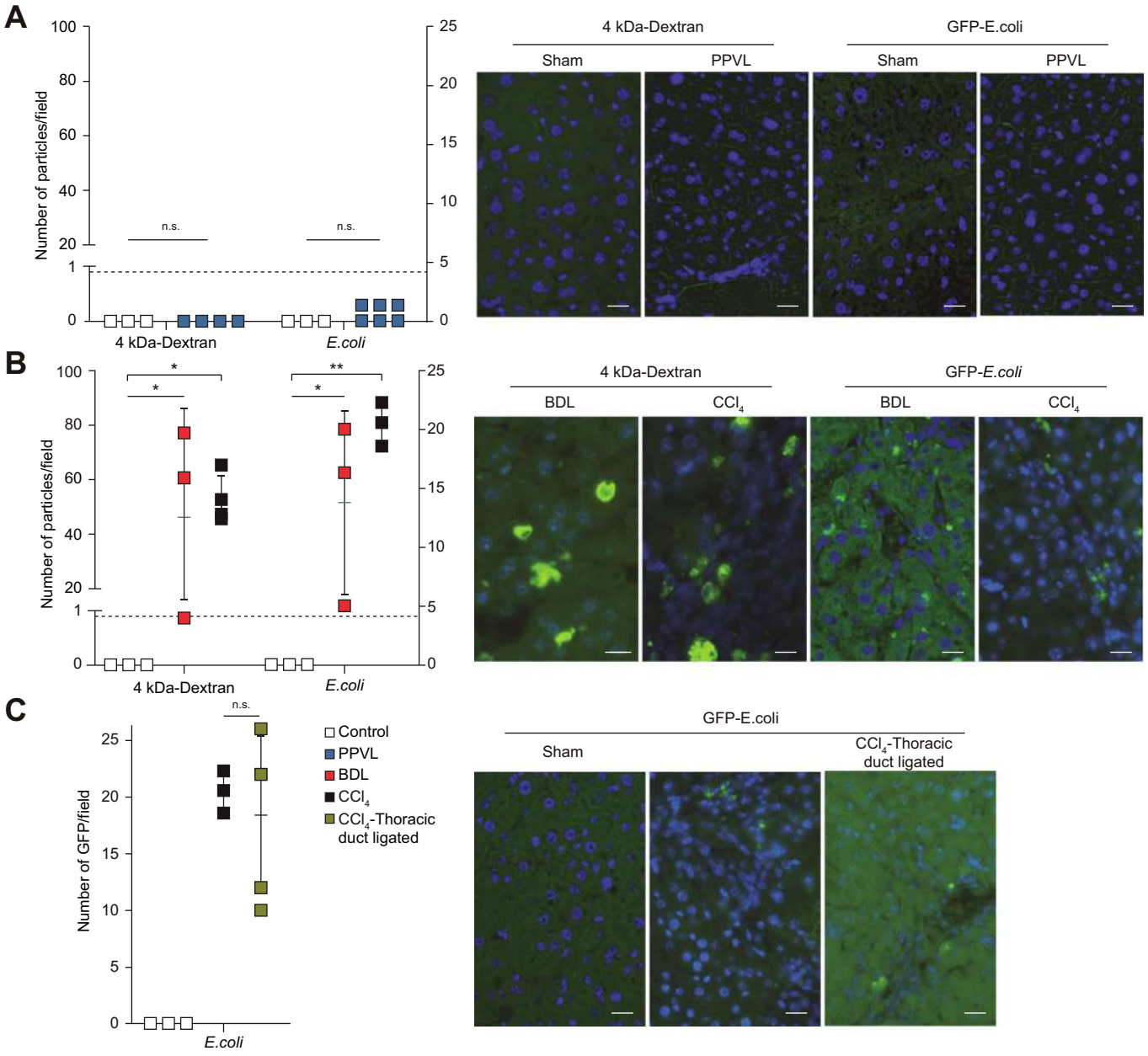

Fig. 1. Pathological translocation via gut-liver axis in cirrhotic but not pre-hepatic portal-hypertensive mice independent from lymphatic route. Liver sections assessed for 4 kDA-FITC-dextran and GFP-*E. coli* in intestinal loop experiments. No detectable fluorescent probe in livers of control or PPVL mice (A). High retrieval rate of FITC- (B) and GFP-signal (C) in livers of BDL and CCl_4-cirrhotic mice were not different in quantity after ligation of the thoracic lymphatic duct. Representative images of A-C are provided on the right. White scale line indicates 20 μm. Colors depicting experimental groups are shown on lower right. Each dot represents the mean counts of at least 10 pictures per animal. Pictures are representative of the indicated experimental groups. $^{*}p$ <0.05, $^{**}p$ <0.01 *vs.* others (Student's *t* test).

augmented in BDL mice (Fig. S2A). Interestingly, the quantity of GFP-*E. coli* translocation to PPs was about 2-fold increased compared to MLNs. Moreover, surprisingly supernatant from PPs but not MLNs contained high numbers of GFP-*E. coli,* indicating cell-independent passage and translocation (Fig. S4C). However, the severity of translocation to MLNs appeared to be less pronounced than the gut-liver axis (Fig. S2B). Internalization analysis shows that the cellular fraction of MLNs and PPs from BDL mice have more GFP internalized than those from healthy controls and PPVL mice (Fig. S4 A,B). The subgroup analysis of GFP-transporting cells revealed the highest frequency among CD11c +/myeloid dendritic cells (Fig. S4 D,E). In addition, in the cellular fraction of MLNs from BDL mice, significantly more neutrophils were observed than in the corresponding evaluation in sham and/or PPVL mice. Analysis of all cellular fractions that do not have GFP internalized (or attached) revealed significantly more neutrophils and CD11c+/myeloid dendritic cells in MLNs and PPs from BDL mice than from healthy controls and/or PPVL mice (data not shown).

Mucus layer is reduced in thickness with loss of GCs and MUC2-expression associated with bacterial overgrowth in inner mucus layer in cirrhotic but not PPVL mice

As the number of GCs is higher in the distal than the proximal portion of the small intestine (data not shown), with the highest numbers in the terminal ileum, we focused on this site for any

Please cite this article in press as: Sorribas M et al. FXR-modulates the gut-vascular barrier by regulating the entry sites for bacterial translocation in experimental cirrhosis. J Hepatol (2019), https://doi.org/10.1016/j.jhep.2019.06.017

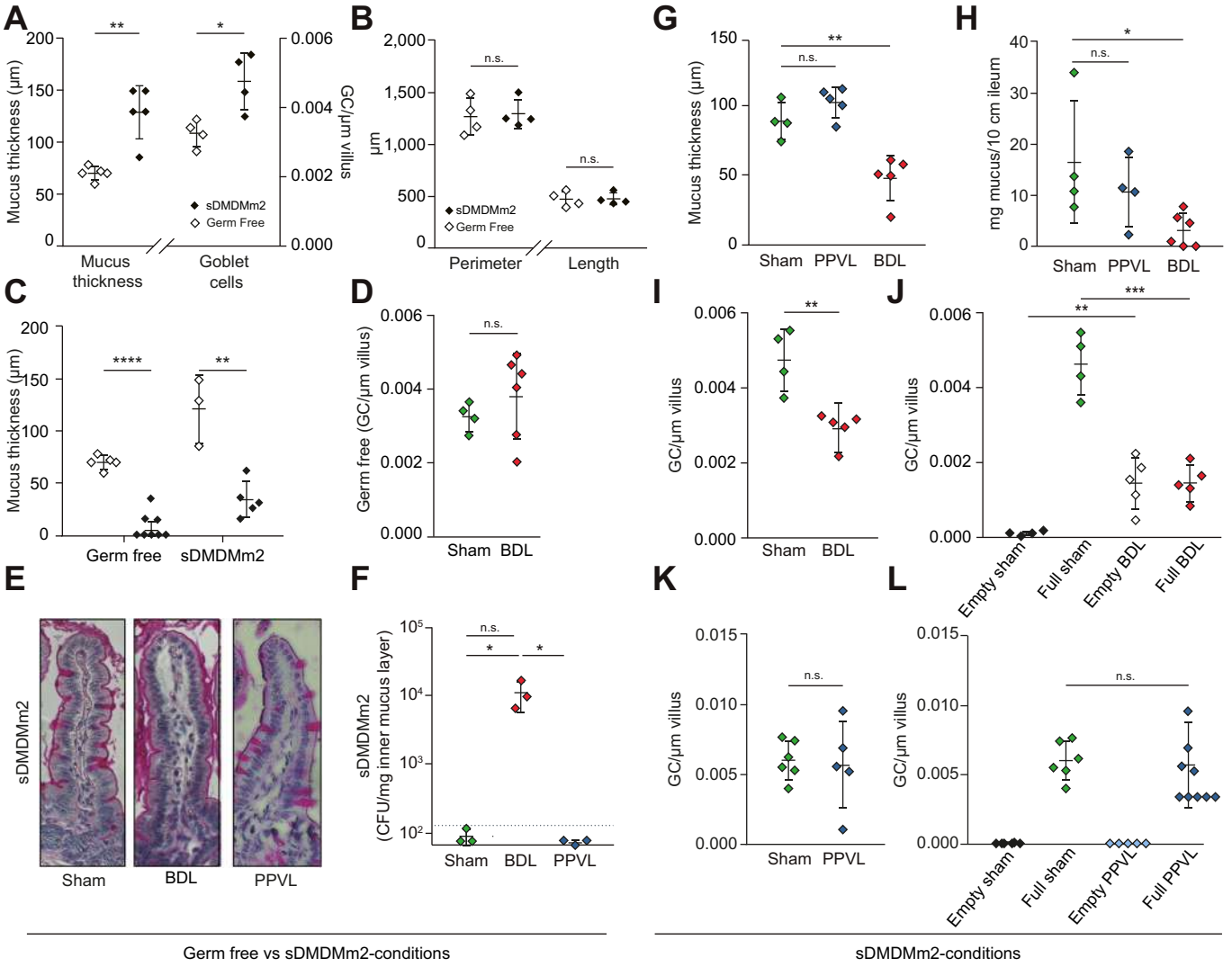

Fig. 2. Impact of microbiota and cirrhosis on ileal mucus layer. Left (germ-free *vs.* sDMDM2). Mucus thickness and GC numbers were reduced in germ-free compared to sDMDM2-colonized mice (A), and differences in GC numbers related predominantly to mucin-filled GCs, as empty GCs were almost absent in germ-free and sDMDM2-conditions (B). In BDL mice (shown by filled symbols), already 3 days after surgery, mucus thickness was reduced in germ-free and sDMDM2-conditions (C), whereas GC numbers were not affected in germ-free conditions (D), but likewise diminished in sDMDM2-conditions (I). In chronic 14 day-PPVL mice in sDMDM2-conditions, no change in mucus thickness (G), mucus weight per segment ileum (H) nor GC numbers (total (L) as well as full and/or empty appearing (M)) was noted. In contrast, BDL mice under sDMDM2-conditions showed increased numbers of empty appearing and reduced mucin-filled GC (J). Representative staining of ileal villus derived from sham, PPVL and BDL are depicted (E). The inner mucus layer revealed vastly increased bacterial overgrowth in this normally sterile layer, as seen in sham and PPVL mice (F). *p <0.05 and **p <0.01. t test; n.s.: non-significant. Each dot represents 1 mouse with a mean of at least 30 villi counted. Mean ± standard deviation (SD) displayed for the indicated experimental groups.

further investigations. We observed a marked reduction in mucus thickness and GC numbers in germ-free mice (Fig. 2A), underlining the role of the microbiota as a stimuli for the mucus compartment. However, villus morphology in terms of length and perimeter was not changed in germ-free conditions (Fig. S5A). Moreover, distribution of GCs along the villus with more numbers per length of villus within the base as compared to the apex as well as almost lack of empty appearing GC was similar in germ-free and colonized mice (Fig. S5B, Fig. 2B). In germ-free conditions, short-term BDL mice (Fig. 2C) presented with reduced mucus thickness. However, BDL mice presented with increased mortality in germ-free conditions (Fig. S6) preventing further investigations. Thus, we utilized an sDMDM2, as a gnotobiotic animal model, consisting of 12 pre-defined bacterial species.[40] This microflora also increased GC counts and mucus thickness in the terminal ileum of healthy mice. In more detail, this increase in GC in response to this more diverse microflora resulted in an increased number of mucin-filled GCs, predominantly in the base of the villus. Cirrhotic mice under sDMDM2-conditions presented with lower mucus thickness, mucus weight per ileum length, and GC numbers in the terminal ileum compared to healthy controls (Fig. 2G,H,I, Fig. S5C), predominantly with a reduction in mucin-filled GCs (Fig. 2J, Fig. S5D). Moreover, BDL-cirrhosis resulted in more than 100x increased bacterial burden in the inner mucus layer (Fig. 2F), evidencing a closing in of bacteria on the epithelial surface, which is normally almost devoid of bacteria. Also, microbial composition changed in BDL mice presenting with increased abundance of particularly *Enterococcus* within the mucus compartment compared to sham mice (Fig. S7). On the other hand, decreased abundance of *Verrucomicrobia* and *Parasutterella* was noted in ileal mucus of BDL mice. Surprisingly,

Please cite this article in press as: Sorribas M et al. FXR-modulates the gut-vascular barrier by regulating the entry sites for bacterial translocation in experimental cirrhosis. J Hepatol (2019), https://doi.org/10.1016/j.jhep.2019.06.017

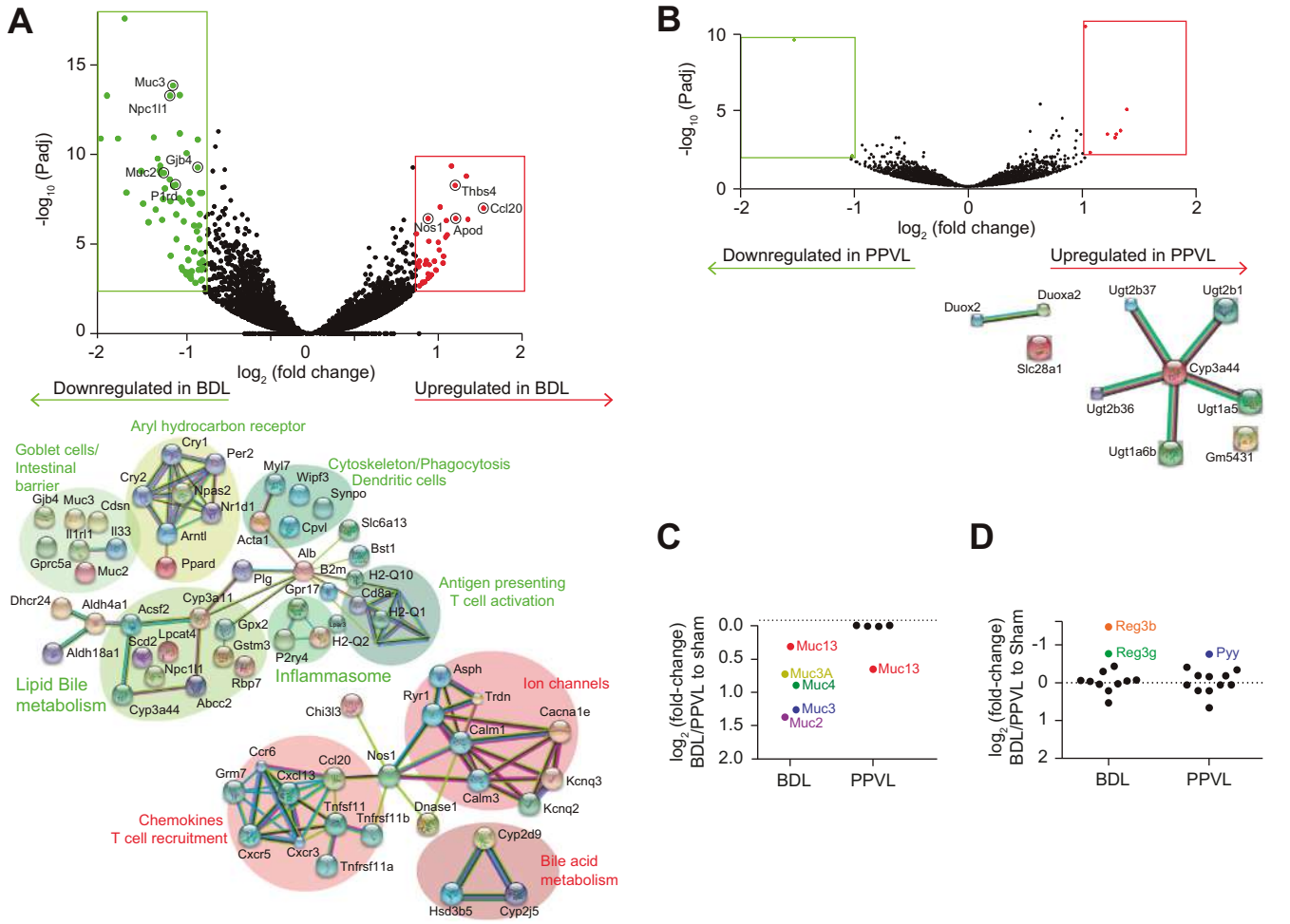

Fig. 3. Volcano plot and string analysis of differently expressed genes in terminal ileum tissue. Results show fold-change of selected transcripts between BDL and sham mice (A) and PPVL (B) *vs.* sham mice. Genes expressed at significantly altered levels are highlighted in red (p-adj <0.01) and genes of interest labeled. String analysis for protein-protein interactions (depicted as connections) is done on differently expressed genes (log2-fold-change >2; p-adj <0.01) (A and B, lower panel, respectively). Logarithmic fold-change in selected transcripts of mucus-synthesis (C) and antimicrobial molecule expression (D) in BDL and PPVL mice in relation to sham-animals. Differentially expressed genes are colored and labeled (p-adj <0.01). The analysis was conducted using mean gene counts of 3 animals per group.

also in pre-hepatic portal hypertension *per se* (in PPVL mice), minor dysbiosis was observable but there was no change in the abundance of *Enterococci* (Fig. S7C).

In cirrhotic mice, those with the lowest mucus thickness within the terminal ileum under sDMDM2-conditions presented with the most pronounced bacterial translocation to the liver (Fig. S5E). Contemporarily, cirrhotic animals with pathological translocation to MLNs or with ascites presented with reduced numbers of GCs (Fig. S5 F,G). This indicates that GC numbers decrease with advanced stages of disease and/or presence of PBT. Under sDMDM2 conditions, total GC count and mucus thickness were not only diminished in long-term and cirrhotic BDL mice, but already 3 days after BDL (Fig. 2C) and hence independent of fibrosis/cirrhosis. In that regard, we observed particularly reduced numbers of full but a trend to more empty GCs (Fig. 2J). In contrast, in germ-free conditions, no change in GC numbers was noted 3 days after BDL (Fig. 2D). As for the role of portal hypertension *per se,* no differences in terms of mucus thickness, mucus weight per segment ileum, or total numbers of GCs, as well as numbers of mucin-filled or empty GCs, were observed in PPVL mice compared to control animals (Fig. 2 G,H,L,M).

RNA sequencing of whole ileal tissue revealed upregulation of genes involved in bile acid metabolism, chemotaxis and T-cell recruitment and downregulation of genes involved in phagocytosis, antigen-presentation, lipid metabolism and GC/intestinal barrier regulation in BDL mice (Fig. 3A). Notably, downregulation of the main mucin-genes (MUC2,-3,-4,-13) was observed, suggesting a lack of mucin-synthesis in ileal GCs in BDL mice (Fig. 3C). In contrast, no changes in mucin-gene-expression (except for MUC13) could be observed in PPVL mice (Fig. 3B, C). However, ileal expression of antimicrobial peptides REG3Band REG3G were upregulated in BDL mice without detectable changes in PPVL mice (Fig. 3D).

Interepithelial leakage and bacterial translocation across the epithelial barrier into the lamina propria are enhanced in cirrhotic but not in pre-hepatic portal-hypertensive mice

Dual-band confocal laserendomicroscopy *in vivo* (Fig. 4), as well as confocal microscopy *ex vivo* (data not shown), evidenced translocation of GFP-*E. coli* from the ileal lumen into the lamina propria in BDL mice. Astonishingly, even at high-concentrations of GFP-*E. coli* within the intestinal loops, no clear translocation of bacteria across the well-visualized epithelial barrier was

Please cite this article in press as: Sorribas M et al. FXR-modulates the gut-vascular barrier by regulating the entry sites for bacterial translocation in experimental cirrhosis. J Hepatol (2019), https://doi.org/10.1016/j.jhep.2019.06.017

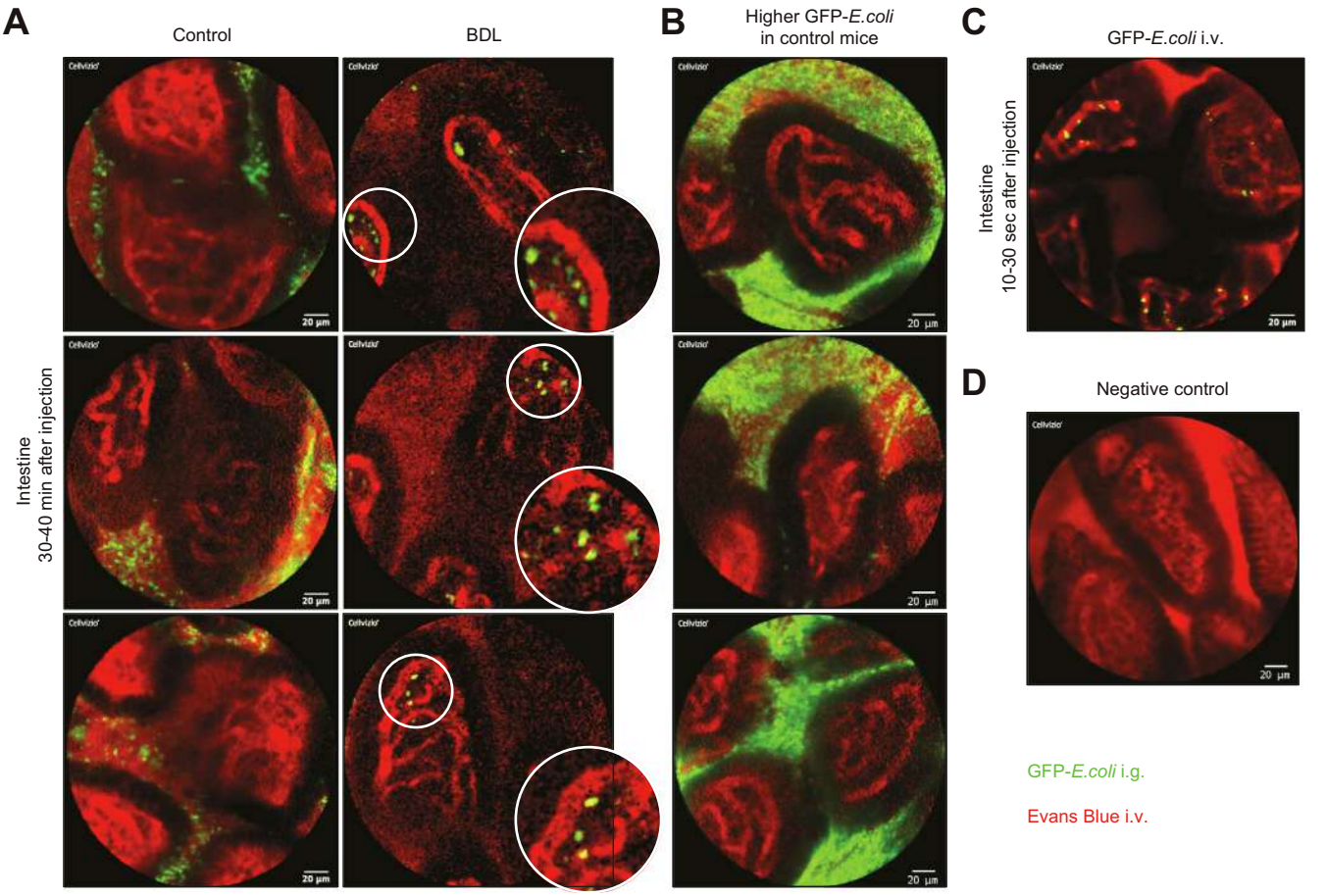

Fig. 4. Pathological transepithelial GFP-*E. coli* translocation into the lamina propria occurs in BDL mice but not in healthy conditions or in PPVL mice. Dual-band laserendomicroscopy *in vivo* in healthy control and BDL mice after injection of GFP-*E. coli* into the intestinal villi of the ileal loop were observed for 60 min *in vivo* showing no GFP-signal in controls but multiple translocating GFP-marked *E. coli* within the lamina propria in BDL mice (A). Bacteria sticking to the outside of capillaries can be seen, with single cases of bacteria having migrated into the vessels depicted. Even at artificially high concentration of GFP-*E. coli* up to 10^8 CFU/loop no transepithelial translocation of bacteria into the lamina propria was observed in healthy controls (B). Positive control displaying GFP-*E. coli* within the vasculature after i.v. injection (C) and negative control without exposition to GFP-*E. coli* (D) are shown as well. Pictures are representative of the indicated experimental groups from 2 replicate experiments.

noted in healthy control mice during the 30 min observation period (Fig. 4B). Interepithelial permeation of 70 kDA- and 150 kDA-FITC-dextran into the ileal epithelial layer was not detectable in any control animal (Fig. 5A,B). In contrast, in cirrhotic (BDL and CCl_4-treated) mice, but likewise not in PPVL mice, interepithelial leakage of 70 kDa-FITC-dextran was observed (Fig. 5A). Correspondingly, PPVL did not show any increase in fecal albumin (66–70 kDA), whereas cirrhotic mice excreted high amounts of albumin demonstrating a disruption of the epithelial barrier (Fig. S8). Large-sized 150 kDA-FITC-dextran did not leak into the interepithelial space, to the degree defined per protocol to indicate epithelial barrier dysfunction in any of the study groups (Fig. 5B).

A semiquantitative analysis of immunohistochemistry revealed the downregulation of main tight junction (TJ) proteins in ileal epithelium including ZO1, occludin and claudin-1,-2 in CCl_4-induced cirrhotic mice compared to naïve control mice (Fig. S9). Cirrhotic mice treated with OCA showed a significant increase in all TJ proteins, either reaching or approaching values present in naïve control mice. Cirrhotic mice treated with Fex showed similar results, significantly increasing protein expression of all TJ proteins, except occludin, compared to untreated cirrhotic mice.

Gut-vascular barrier dysfunction in cirrhotic but not pre-hepatic portal-hypertensive mice is independent of intestinal microbiota

In healthy control animals under SPF conditions we could clearly see that 4 kDa-FITC- dextran extravasated immediately after injection into the lamina propria (Suppl. Video 1), while 40 kDa stayed transiently in the vessel but leaked progressively through the endothelium within the first 3 to 5 min, reaching a 1:1 ratio after around 10 min (Fig. 6B). 70 kDa Dextran-FITC could stay in the vessel for up to 8 min, staining capillaries and giving contrast between vessels and lamina propria, although also extravasated between 5 and 20 min. Finally, 150 kDa-Dextran-FITC remained intravascular for all the observation (30 min) in control mice (Fig. 6B). Ileal vascular permeability was increased in cirrhotic (BDL and CCl_4) mice with early and enhanced extravasation of 70 kDA (Fig. 6E) and 150 kDa-FITC-dextran (Fig. 6F) compared to control mice. In contrast, like sham mice, none of the PPVL mice presented with augmented leakage of 150 kDa-FITC-dextran (Fig. 6F). Almost identical kinetics and severity of leakage of pre-defined FITC-dextrans were observed in germ-free control mice compared to SPF conditions (Fig. 6A,B). Namely, small-sized 4 kDA- and 40 kDA-FITC-dextrans permeated early and severely, whereas

Please cite this article in press as: Sorribas M et al. FXR-modulates the gut-vascular barrier by regulating the entry sites for bacterial translocation in experimental cirrhosis. J Hepatol (2019), https://doi.org/10.1016/j.jhep.2019.06.017

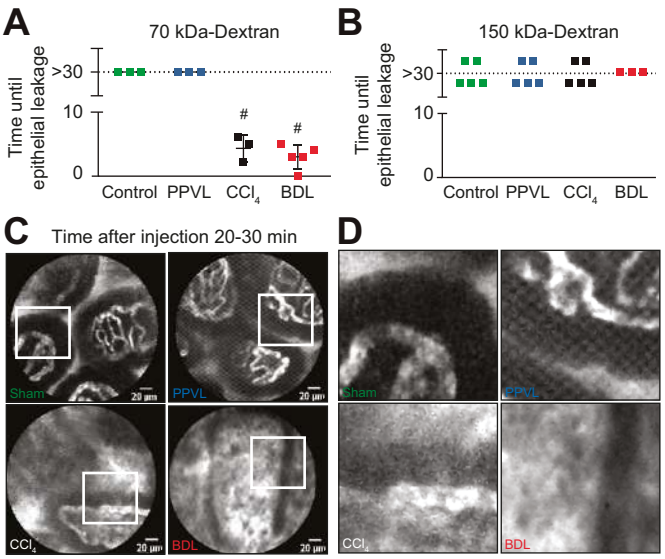

Fig. 5. Interepithelial leakage of fluorescein is increased in experimental cirrhosis. Pathological interepithelial appearance of 70 kDA-FITC-dextran (A) but not 150 kDA-FITC-dextran (B) in ileal villi in cirrhotic BDL and CCl_4-treated but not in PPVL- and healthy control mice, assessed by probe-based confocal laser endomicroscopy *in vivo*. Representative images from confocal laser endomicroscopy are depicted at the stated observation time points (C) and corresponding magnifications of inlets (D). $^{***}p$ <0.001 *t* test. Each dot represents the mean counts of at least 8 pictures per animal and timepoint, the experiment was done at least 3 times. Pictures are representative of the indicated experimental groups and timepoints.

large-sized 150 kDA-FITC-dextran remained intravascularly during the whole observation period. Only 70 kDA-FITC-dextran extravasated earlier and more severely in germ-free compared to SPF-mice. Short-term BDL mice in germ-free conditions presented with vastly disrupted GVB, exhibiting rapid and severe extravasation of even large-sized 150 kDA-FITC-dextran (Fig. 6 C,D).

Increased PV1-expression and changes in endothelial cell morphology correlate with disrupted GVB in cirrhosis

Ileal GVB impairment was associated with increased PV-1 expression along the gastrointestinal tract. Interestingly, gut vascular analysis in terms of immunofluorescence for PV-1 expression showed increased staining in all small and large bowel locations, in CD34-positive vessels in cirrhotic BDL mice (Fig. 7A,B). However, PPVL mice displayed minor enhancement in the ileum and significant increases in the colon compared to sham mice (Fig. 7 C,D). Electron microscopy revealed no major changes in the number of fenestrae, caveolae or perimeter of capillaries assessed in cirrhotic or pre-hepatic portal-hypertensive capillaries (Fig. 8A-C). However, morphologically endothelial fenestrae appeared enlarged and inter-cellular membranes reduced in electrodensity in cirrhotic ileal capillaries (Fig. 8D).

Role of FXR for ileal mucus and gut-vascular barrier and thus pathological translocation along the gut-liver axis

Oral treatment with OCA, as well as Fex, significantly ameliorated pathological translocation of GFP-*E. coli* from the ileal lumen to the liver in cirrhotic mice (Fig. 9A,B), underlining the impact of pharmacological FXR activation on "sealing" the access to the gut-liver axis. However, none of $Fxr^{\Delta IEC}$ mice analyzed showed any translocation of even small 4 kDa FITC-dextran or GFP-*E. coli* to the liver (data not shown). In contrast, performing PPVL on $Fxr^{\Delta IEC}$ mice led to a small but evident increase in intrahepatically recoverable 4 kDa FITC-dextran, which was not observed in wild-type PPVL mice (Fig. 9 C,D). Also, in individual PPVL-$Fxr^{\Delta IEC}$–mice, GFP-*E. coli* was retrievable intrahepatically (data not shown).

Immunohistochemistry for FXR in the ileum revealed that FXR was not expressed in VillinCre$^{+/-}$ $Fxr^{fl/fl}$ mice (VillinCre $Fxr^{fl/fl}$ in figure legends), but it was expressed in epithelial cells in Villin$^{-/-}$ $Fxr^{fl/fl}$ (wild-type in figure legends) (Fig. S10). FXR was expressed in all enterocytes but was absent in the nuclei of all PAS-positive mucin-filled GCs (Fig. S10). Interestingly we also observed a gradual reduction of FXR expression from the apex of the villus, where the expression was higher, to the base of the crypt. This absence of FXR expression is specifically more pronounced at the base of the crypt in which stem cells and Paneth cells are located and the highest concentration of GCs is found.

As for the muco-epithelial barrier, OCA-treatment partly restored GC numbers in cirrhotic animals to levels not statistically different from control animals (Fig. S10). In addition, OCA significantly increased ileal TJ protein expression (ZO1, claudin-1,-2 and occludin), upregulating them to the level of healthy control mice (Fig. S9). Likewise, Fex improved TJ protein immunohistochemical staining (Fig. S9), but failed to improve GVB when challenged with 70 kDA-FITC-dextran (Fig. 9H) in CCl_4-mice. In contrast, endothelial FXR stimulation, by OCA, at least partly attenuated GVB dysfunction in cirrhotic mice (Fig. 9G).

Discussion

In this paper we report changes in mucus- and GVB in relation to microbial modulation and as entry sites for PBT along the gut-liver axis in cirrhosis. Standardized *in vivo* intestinal loop experiments are utilized to quantify the translocation process from the intestinal lumen to the liver. Pathological increases in bacterial translocation are evidenced in cirrhotic mice, occurring largely independently of the lymphatic route. This does not exclude the well-known PBT along the lymphatic route in cirrhosis, as demonstrated by us[14,41] and multiple other independent investigators.[42–44] Herein, we confirm this in BDL mice and extend this observation by demonstrating a particularly pronounced PBT into PPs, which appears to involve mainly myeloid dendritic cells but also represents at least partly a cell-independent passage and translocation process. However, translocation into the lymphatic system is a physiological event occurring in healthy conditions via a highly orchestrated process at low rates. In contrast, herein, we show that no bacterial and/or 4 kDA-dextran-translocation is detectable intrahepatically in control and pre-hepatic portal-hypertensive mice. This strongly argues for a tight sealing and protection of the gut-liver axis from any bacterial translocation in healthy conditions, which is not significantly altered by portal hypertension. However, in cirrhosis with PBT, the gut-liver axis is markedly "opened" and fueled with bacteria via the intestinal microcirculation and portal-venous route, which seems to represent the predominant route of access to the host.

We chose the distal ileum as the main target site for investigations due to the most drastic increase of bacterial load and the presence of a thinner and more penetrable mucus layer com-

Please cite this article in press as: Sorribas M et al. FXR-modulates the gut-vascular barrier by regulating the entry sites for bacterial translocation in experimental cirrhosis. J Hepatol (2019), https://doi.org/10.1016/j.jhep.2019.06.017

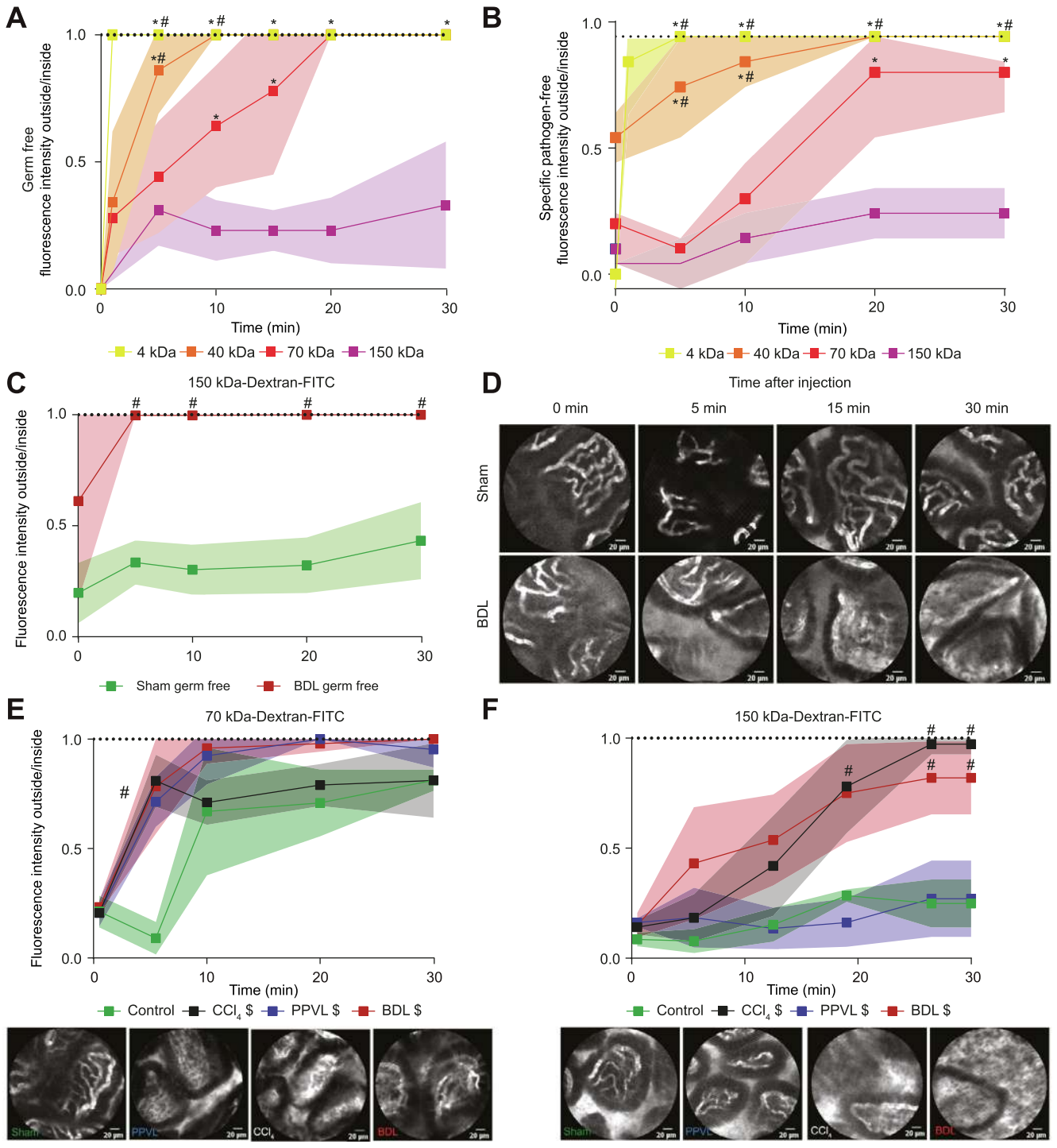

Fig. 6. Gut-vascular barrier function in dependency on microbiota and its disruption in cirrhotic mice. Upper panel: Extravasation of different sized FITC-dextran molecules during 30 min observation period in healthy germ-free (A) and SPF-mice (B). Very similar extravasation kinetics can be seen for 4, 40 and 150 kDA-FITC-dextran in germ-free and SPF-mice. BDL mice born and raised germ-free exhibited grossly accelerated and severe extravasation of 150 kDA-FITC-dextran, which was not observed at all in sham mice (C). Representative images at the stated timepoints in germ-free BDL or sham mice (D). Lower panel: Gut-vascular barrier dysfunction for 70 kDA-FITC-dextran (E) and 150 kDA-FITC-dextran (F) in terminal ileum of cirrhotic and pre-hepatic portal-hypertensive mice. Statistics: One-way ANOVA corrected by Bonferroni $^{*}p$ <0.05 compared to 150 kDa; $^{\#}p$ <0.05 compared to 70 kDa. $^{\$}$Area under the curve significantly different compared to control (*t* test: p <0.05). Each dot represents the mean counts of at least 8 pictures per animal and timepoint, the experiment was done once. Pictures are representative of the indicated experimental groups and timepoints.

pared to the large intestine.[45] Nonetheless, also in the ileum, the mucus layer represents the first line of defense against bacterial translocation with mucus release keeping bacteria at a distance from the epithelium.[13] Correspondingly, defects in mucus barrier function result in increased bacterial adhesion to the surface epithelium and increased intestinal mucosal

Please cite this article in press as: Sorribas M et al. FXR-modulates the gut-vascular barrier by regulating the entry sites for bacterial translocation in experimental cirrhosis. J Hepatol (2019), https://doi.org/10.1016/j.jhep.2019.06.017

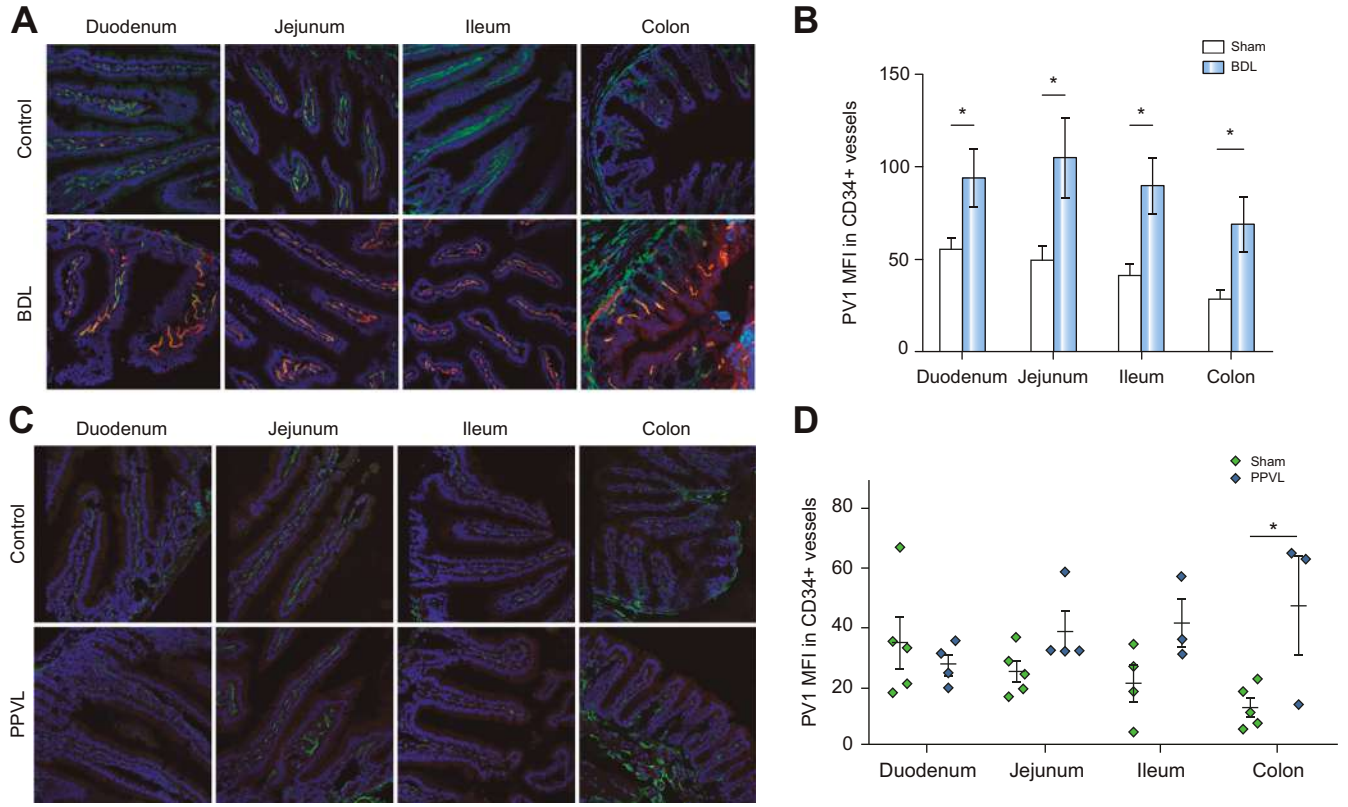

Fig. 7. Plasmalemma vesicle-associated protein 1 immunofluorescence in terminal ileum is increased in cirrhotic but only mildly accentuated in PPVL mice. PV-1 (red) and CD34 (green) staining was performed in different parts of the small intestine (Duodenum, Jejunum, Ileum, and Colon) in BDL (A) and PPVL (C) mice. Quantification of PV-1 fluorescent intensity in CD34 vessels revealed increased staining of PV1 along the small intestine in cirrhotic BDL mice compared to healthy controls (B). In contrast, in PPVL mice, a minor but consistent increase in PV1 at the ileum and particularly colon was detectable (D). One-way ANOVA corrected by Bonferroni: $^*p$ <0.05 (A). *t* test: n.s. – non-significant. Each dot represents the mean counts of at least 5 pictures per animal.

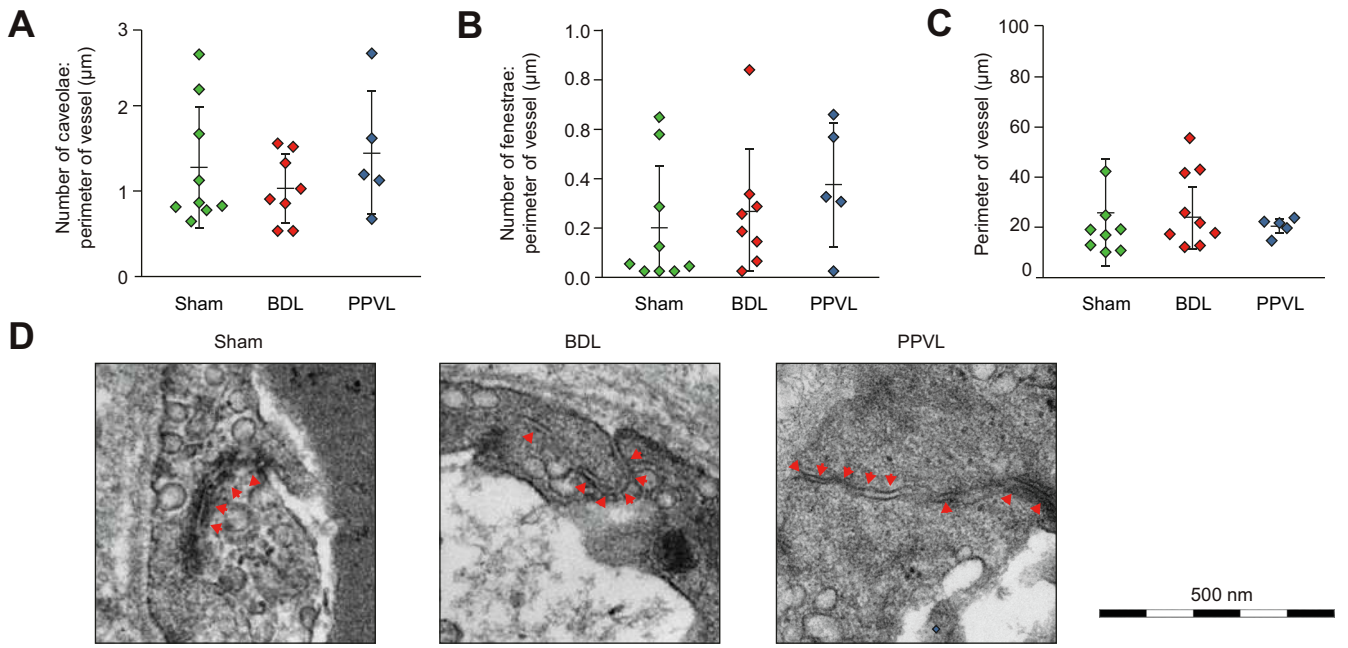

Fig. 8. Morphological characteristics of endothelial cells within the ileal microvasculature in BDL cirrhotic and PPVL mice. Number of caveolae (A) and fenestrae (B) and vessel perimeter (C) are measured in ileal villus capillaries in BDL-induced cirrhotic mice, PPVL and sham-operated control mice. Each dot or column of dots represent 1 vessel measured in 1 mouse, respectively (n = 2 Sham, n = 2 BDL, n = 1 PPVL) (A). Representative electron microscopy pictures showing reduced junctional overlapping (red arrow heads) in portal-hypertensive mice (D).

Please cite this article in press as: Sorribas M et al. FXR-modulates the gut-vascular barrier by regulating the entry sites for bacterial translocation in experimental cirrhosis. J Hepatol (2019), https://doi.org/10.1016/j.jhep.2019.06.017

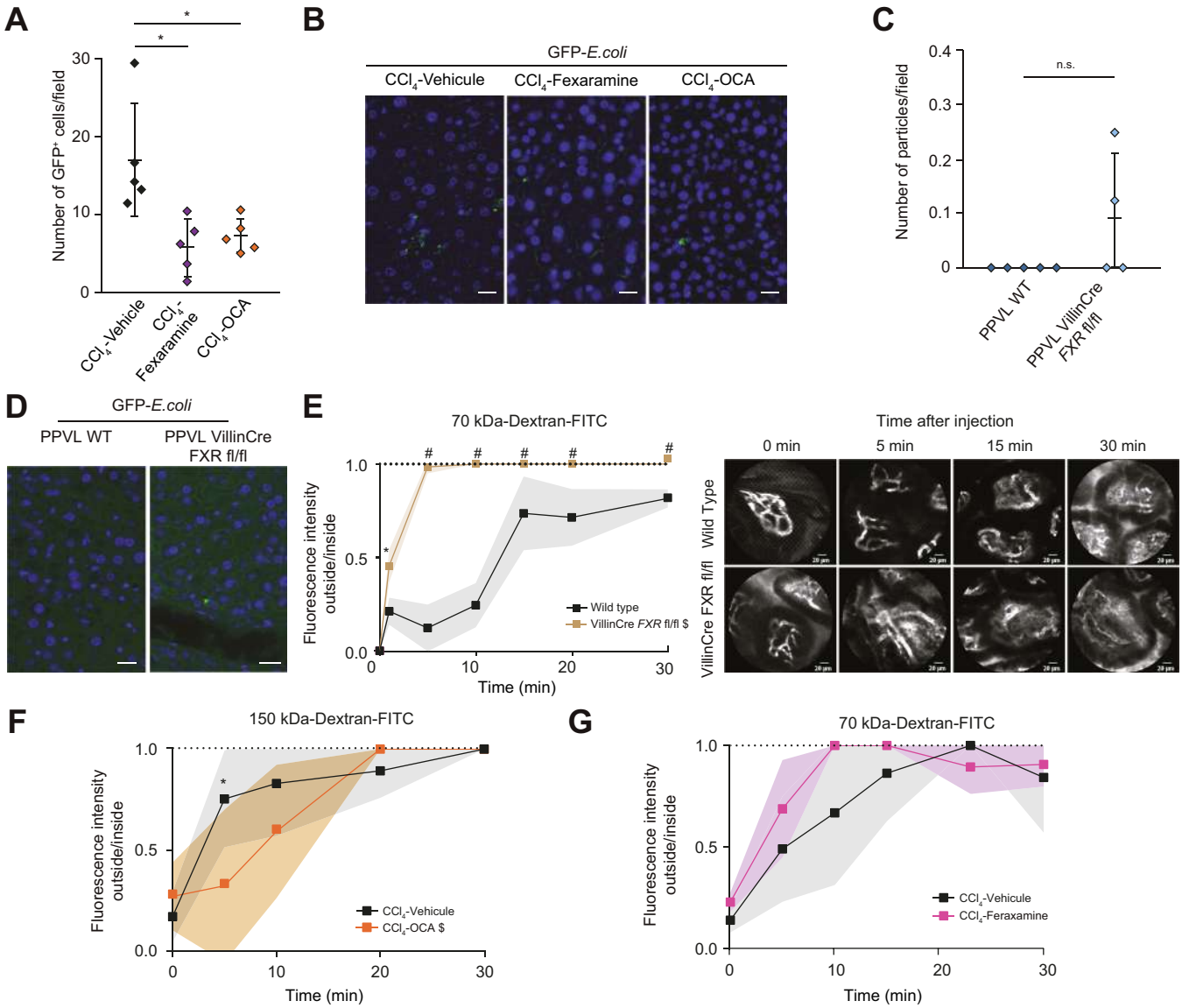

Fig. 9. Role of FXR for gut-liver axis and gut-vascular barrier. Upper panel: FXR-agonists fexaramine and obeticholic acid reduced hepatic recovery of luminally applied GFP-*E. coli* (A,B). Quantification of number of bacteria cells in liver sections per field of view 0.5 mm^2. Each dot represents 1 mouse. Mean ± SD (A,C). Representative pictures of the indicated groups. GFP-*E. coli* (Green) DAPI (blue). White scale lines indicate 20 μm (B,D). CCL_4-induced cirrhotic mice treated for 2 weeks with fexaramine or obeticholic acid orally (A,B). PPVL assessed 14 days after surgery in wild-type and intestinal-specific *Fxr*-null-mice (C,D). One-way ANOVA corrected by Bonferroni: $^{*}p$ <0.05. Lower panel: Gut-vascular barrier disruption and stabilization in dependency on FXR-signaling. In intestinal-specific FXR-deficient mice, GVB is disrupted as 70 kDA-FITC-dextran extravasation occurs earlier and more severely in mice with epithelial-specific deletion of FXR in the intestine than in wild-type-mice (E, G). OCA treatment delayed and initially reduced 150-kDA-FITC-dextran extravasation in mice with CCl_4-induced cirrhosis (F). In contrast, even 70 kDA-FITC-dextran extravasation was not altered by fexaramine-treatment (H). One-way ANOVA corrected by Bonferroni: $^{\#}p$ <0.001 $^{*}p$ <0.05. *t* test of AUC comparison: $^{\$}p$ <0.05.

permeability.[46,47] Colonization of the gastrointestinal tract with microbial commensals has been reported to impact on the intestinal mucus machinery, as well as vascular development. It has many crucial roles, including on normal development of the mucus barrier[31] and on induction of mucus secretion. It also leads to an increasing number of GCs via activation of toll-like receptors in the intestinal epithelium by microbial-derived products.[48] GCs have been studied in germ-free conditions before and found to be reduced in numbers and smaller in size in the cecum compared to conventionally raised mice.[49] Here, we extend this observation for another site, namely small intestine and sDMDM2-gnotobiotic conditions, demonstrating increased total numbers of GCs, particularly mucin-filled GCs, compared to germ-free mice. Moreover, several members of the microbiota community have been reported to increase *Muc2* gene expression *in vivo* and *in vitro* and to release the otherwise membrane-anchored MUC2 molecule.[50] Here we demonstrate under sDMDM2-gnotobiotic conditions reduced mucus thickness and expression of the main mucus- genes in cirrhotic mice. This associates with bacterial overgrowth in the inner mucus layer, which is normally sterile, promoting pathological crossing of *E. coli* into the lamina propria. Most translocation of living bacteria to the liver is seen in mice with low mucus thickness and cirrhotic mice with translocation to the MLNs, present with a reduction in GC numbers compared to those without bacterial translocation. Thus, changes in mucus

Please cite this article in press as: Sorribas M et al. FXR-modulates the gut-vascular barrier by regulating the entry sites for bacterial translocation in experimental cirrhosis. J Hepatol (2019), https://doi.org/10.1016/j.jhep.2019.06.017

parameters can, at least partly, be explained by the observed reduction in GCs with a particularly pronounced reduction in the number of mucin-filled GCs and concomitant increase in empty GCs in liver cirrhosis under standardized gnotobiotic conditions. Surprisingly, a lack of luminal intestinal bile induced by short-term BDL in the absence of microbiota failed to impact on GC density. This hints at the microbiome being responsible for the observed changes in sDMDM2-conditions. Thus, we analyzed ileal microbial composition in mucus, demonstrating changes in microbial clustering with overgrowth of *Enterococcus faecalis* in BDL mice. Considering the mucus-binding as well as mucus degradation capacity of *Enterococci*,[51,52] it is tempting to speculate that this drastic increase in *Enterococci* might actually contribute to the observed reduction in mucus thickness in these animals. More interestingly, these data shed new light on the most recent demonstration of *Enterococcus* overgrowth in gastric acid depleted conditions and associated progression of alcohol-related liver disease.[53] Indeed, in conjunction with the observed protection of *Muc2*-deficient mice from alcohol-related liver disease,[54] the mucus niche is a highly attractive target for preventive and/or therapeutic modulation in liver diseases. However, further studies need to address this, as well as the exact role of bile acids, on the observed changes.

Microbial commensals of the gastrointestinal tract have been implicated in the development of the intricate network of blood capillaries in intestinal villi, at least partly depending on angiogenic factors secreted by Paneth cells.[32] More interestingly monocolonization with *Bacteroides thetaiotaomicron* a common human and mouse gut commensal is enough to promote vascular development. In line with these results, we have also shown that transient bacterial colonization with the reversible auxotrophic *E. coli* strain HA107 is enough to induce angiogenic genes and increase vascular density within the intestinal villi.[55] As for vascular barrier function, we demonstrate that the microbiome is of rather limited impact. In fact, germ-free mice present with similar permeation characteristics for small and large-sized molecules as mice with normal gut flora. However, a modulatory role for microbes and microbial products cannot be excluded considering the observed expedited leakage of pathological sized molecules in BDL mice in germ-free conditions. This indeed hints towards some protective effects of the microbiome in stabilizing the GVB. In fact, also for 70 kDA-dextran, resembling albumin in size, extravasation is slower in the presence of a complex microbiome compared to germ-free conditions. Thus, the microbiome appears to be of major relevance for the mucus machinery but, despite exerting some impact, GVB permeability appears to be relatively unaffected.

Vascular changes in the splanchnic circulation have been characterized intensively in terms of compliance, hemodynamic dysregulation and angiogenesis, but only limited data are available for endothelial permeability. The newly described GVB is grossly disrupted in cirrhotic mice (BDL, CCl_4) with rapid extravasation of large-sized molecules (150 kDA) more than twice the size of albumin. Concomitantly, enteral loss of albumin is observed in cirrhotic conditions but not in pre-hepatic portal hypertension. This is in accordance with the lack of interepithelial fluorescence detectable for 70 kDA-FITC-dextran in PVL-mice, considering albumin is 66 kDA in size and known to leak predominantly paracellularly. The expedited extravasation of large-sized molecules from intestinal capillaries in cirrhotic mice easily explains the well-known edema within the lamina propria, caused by concomitant fluid shifts and increases in interstitial pressures. Vascular hyperpermeability in cirrhotic mice did associate with augmented PV-1 availability, known as a biomarker for the level of endothelial permeability.[56] This is in line with our previous observation of increased expression of PV1 and intestinal endothelial permeability during a high-fat diet and disruption of the GVB.[57] The exact mechanisms upregulating PV1-availability in cirrhosis need to be delineated but could involve endothelial growth factor-A (VEGF). Indeed, PV1 has been reported to be upregulated by VEGF[58] and inhibition of PV1 expression resulted in decreased VEGF-induced endothelial permeability of fluorescent tracers, both *in vivo* and *in vitro*.[59] Considering the well-known increased serum levels of VEGF in experimental cirrhosis, it is tempting to speculate that this contributes to the observed PV1 upregulation.

As for the underlying mechanism of PBT to the liver, we propose that the muco-epithelial and vascular endothelial barrier need to be disrupted simultaneously in order to allow permeation from the lumen into the portal-venous circulation, such as in liver cirrhosis but not in pre-hepatic portal hypertension. Indeed, portal hypertension *per se,* in the absence of liver injury, fails to induce alterations in mucus thickness, weight per ileum length, MUC2-expression and GC numbers. In addition, increased portal pressure alone does not associate with permeation of *E. coli* trans-mucoepithelially into the lamina propria. Moreover, although GVB is disrupted to some degree, permeability is limited to small-/medium-sized molecules of up to 70 kDA. However, in the presence of a second hit known to affect the epithelial barrier (such as a lack of epithelial FXR-signaling), this minor alteration is sufficient to enable some access to the villus microcirculation for molecules that normally do not permeate the vascular endothelium. Indeed, $Fxr^{\Delta IEC}$ mice *per se* do not present with either 4 kDA-FITC-dextran or GFP-*E. coli* translocation to the liver but, once PPVL is performed and GVB is disrupted, the gut-liver axis is fueled and 4 kDA-FITC and *E. coli* appear intrahepatically.

Thus, FXR appears to play a central role in the modulation of both barriers, explaining the therapeutic benefit of systemic and/or local intestinal FXR activation established in experimental cirrhosis. Both FXR-agonists, OCA and Fex abrogated pathological *E. coli* translocation to the liver, underlining their effect in "sealing" the gut-liver axis. FXR-agonists have been used before in experimental portal hypertension.[15,43,60,61] However, direct assessment of their effectiveness on the gut-liver axis is lacking. OCA has been reported to lower intrahepatic resistance, ameliorating portal hypertension,[60,61] while FXR activation in the small intestine reduces bacterial translocation to MLNs in experimental cirrhosis[15,43] and acute cholestasis.[62] However, the mode of action in our experiments, as for the gut-liver axis, appears independent from portal hypertension and not influenced by lymphatic drainage. Hence, overall, we present a new modulatory role of FXR for mucus and GVB affecting the gut-liver axis.

FXR activation by OCA, as well as Fex, increased ileal protein expression of the main TJ proteins (ZO1, occluding, claudin-1, -5) in cirrhotic mice. This is in line with previous reports demonstrating that FXR activation influences intestinal epithelial cell proliferation and apoptosis,[25] increases ileal ZO1-expression[15] and exerts potent anti-inflammatory actions in the intestine, stabilizing epithelial integrity.[26,63,64] Herein, we report, in addition, that OCA impacted on the mucus machinery by increasing ileal GC numbers in cirrhotic animals to a level similar to control mice. Moreover, the fact that 3 days after

Please cite this article in press as: Sorribas M et al. FXR-modulates the gut-vascular barrier by regulating the entry sites for bacterial translocation in experimental cirrhosis. J Hepatol (2019), https://doi.org/10.1016/j.jhep.2019.06.017

BDL, in absence of liver fibrosis/cirrhosis, mucus thickness is reduced, and the numbers of GCs are decreased, supports a role for bile salts in GC homeostasis. In conjunction, with the well-known deficiency in luminal availability of bile acids[24] and associated reduction in ileal FXR-signaling in cirrhotic rodents,[15] it is tempting to speculate that deficient bile acid-induced FXR-signaling could mediate this phenotype. However, we were unable to detect FXR expression in GCs, suggesting a paracrine mode of action for bile acids, which needs to be delineated in further studies.

On the vascular side, FXR has been shown to be expressed on endothelial cells[65] and we have reported previously that specific FXR deletion in endothelial cells disrupts the GVB, leading to liver damage in high-fat diet models.[57] Here, we extend these data by demonstrating stabilization of the dysfunctional GVB in cirrhotic animals given the systemically active FXR agonist, OCA. In contrast, Fex failed to impact on the GVB. The latter indicates that improvements in each barrier separately can be sufficient to block PBT to the liver.

In summary, the microbiota appears key to mucus- and GC physiology, whereas its impact on GVB function seems rather limited. Access to the gut-liver axis in healthy conditions, with normal gut flora, is highly regulated and restricted in size and quality. In contrast, pathological translocation to the liver develops in cirrhosis independently of portal hypertension and the lymphatic route. This opening of the gut-liver axis associates with mucus- and GVB dysfunction modulated at least partly by FXR. OCA and Fex both reduce PBT in cirrhosis but acting differently at the muco-epithelial and the vascular endothelial barrier.

Financial support
This work was supported by Swiss-National-Fund SNF 310030_152805 to RW and SNF 31003A_163143 to ADG.

Conflict of interest
The authors declare no conflicts of interest that pertain to this work.

Please refer to the accompanying ICMJE disclosure forms for further details.

Authors' contributions
M.S. ideated and performed the experiments; M.J., D.S., Y.N., S. M., M.H. helped M.S. in the execution of the mouse experiments; B.Y. and L.H. performed microbial analysis; M.R. provided human investigations and administered the informed consents; A.G., M.R., A.A. participated with ideas, results interpretation, and careful reading of the manuscript; R.W. ideated the study, coordinated the work, and wrote the manuscript.

Acknowledgements
The intestine-specific *Fxr*-null ($Fxr^{\Delta IE}$) mice were a kind gift of Prof. B. Schnabl (University of San Diego, CA, USA); Electron microscopy sample preparation and imaging were performed with devices supported by the Microscopy Imaging Center (MIC) of the University of Bern. We greatly appreciate technical support by F. Blank and C. Wotzkow from Department Pneumology and Department for Biomedical Research, University of Bern, Bern, Switzerland.

Supplementary data
Supplementary data to this article can be found online at https://doi.org/10.1016/j.jhep.2019.06.017.

References
[1] Wiest R, Albillos A, Trauner M, Bajaj JS, Jalan R. Targeting the gut-liver axis in liver disease. J Hepatol 2017;67:1084–1103.
[2] Wiest R, Garcia-Tsao G. Bacterial translocation (BT) in cirrhosis. Hepatology 2005;41:422–433.
[3] Jalan R, Fernández J, Wiest R, et al. Bacterial infections in cirrhosis: a position statement based on the EASL Special Conference 2013. Consensus Development Conference presented at Journal of hepatology; Jun, 2014.
[4] Garcia-Tsao G, Wiest R. Gut microflora in the pathogenesis of the complications of cirrhosis. Best Pract Res Clin Gastroenterol 2004;18:353–372.
[5] Wiest R, Lawson M, Geuking M. Pathological bacterial translocation in liver cirrhosis. J Hepatol 2014;60:197–209.
[6] Spadoni I, Zagato E, Bertocchi A, et al. A gut-vascular barrier controls the systemic dissemination of bacteria. Science (New York, NY) 2015;350:830–834.
[7] Johansson ME, Sjovall H, Hansson GC. The gastrointestinal mucus system in health and disease. Nat Rev Gastroenterol Hepatol 2013;10:352–361.
[8] Johansson ME, Phillipson M, Petersson J, Velcich A, Holm L, Hansson GC. The inner of the two Muc2 mucin-dependent mucus layers in colon is devoid of bacteria. PNAS 2008;105:15064–15069.
[9] Li H, Limenitakis JP, Fuhrer T, et al. The outer mucus layer hosts a distinct intestinal microbial niche. Nat Commun 2015;6:8292.
[10] Johansson ME. Fast renewal of the distal colonic mucus layers by the surface goblet cells as measured by in vivo labeling of mucin glycoproteins. PLoS ONE 2012;7 e41009.
[11] Knoop KA, McDonald KG, McCrate S, McDole JR, Newberry RD. Microbial sensing by goblet cells controls immune surveillance of luminal antigens in the colon. Mucosal Immunol 2015;8:198–210.
[12] Birchenough GM, Johansson ME, Gustafsson JK, Bergstrom JH, Hansson GC. New developments in goblet cell mucus secretion and function. Mucosal Immunol 2015;8:712–719.
[13] Birchenough GM, Nystrom EE, Johansson ME, Hansson GC. A sentinel goblet cell guards the colonic crypt by triggering Nlrp6-dependent Muc2 secretion. Science (New York, NY) 2016;352:1535–1542.
[14] Wiest R, Das S, Cadelina G, Garcia-Tsao G, Milstien S, Groszmann RJ. Bacterial translocation in cirrhotic rats stimulates eNOS-derived NO production and impairs mesenteric vascular contractility. J Clin Investig 1999;104:1223–1233.
[15] Ubeda M, Lario M, Munoz L, et al. Obeticholic acid reduces bacterial translocation and inhibits intestinal inflammation in cirrhotic rats. J Hepatol 2016;64:1049–1057.
[16] Schierwagen R, Alvarez-Silva C, Madsen MSA, et al. Circulating microbiome in blood of different circulatory compartments. Gut 2018.
[17] Wiest R. Splanchnic and systemic vasodilation: the experimental models. J Clin Gastroenterol 2007;41:S272–287.
[18] Wiest R, Tsai MH, Groszmann RJ. Octreotide potentiates PKC-dependent vasoconstrictors in portal-hypertensive and control rats. Gastroenterology 2001;120:975–983.
[19] Castro A, Jimenez W, Claria J, et al. Impaired responsiveness to angiotensin II in experimental cirrhosis: role of nitric oxide. Hepatology 1993;18:367–372.
[20] Fernandez M, Semela D, Bruix J, Colle I, Pinzani M, Bosch J. Angiogenesis in liver disease. J Hepatol 2009;50:604–620.
[21] Rahimi N. Defenders and challengers of endothelial barrier function. Front Immunol 2017;8:1847.
[22] Stan RV, Tkachenko E, Niesman IR. PV1 is a key structural component for the formation of the stomatal and fenestral diaphragms. Mol Biol Cell 2004;15:3615–3630.
[23] Stan RV, Tse D, Deharvengt SJ, et al. The diaphragms of fenestrated endothelia: gatekeepers of vascular permeability and blood composition. Dev Cell 2012;23:1203–1218.
[24] Schwartz CC, Almond HR, Vlahcevic ZR, Swell L. Bile acid metabolism in cirrhosis. V. Determination of biliary lipid secretion rates in patients with advanced cirrhosis. Gastroenterology 1979;77:1177–1182.
[25] Maran RR, Thomas A, Roth M, et al. Farnesoid X receptor deficiency in mice leads to increased intestinal epithelial cell proliferation and tumor development. J Pharmacol Exp Ther 2009;328:469–477.

Please cite this article in press as: Sorribas M et al. FXR-modulates the gut-vascular barrier by regulating the entry sites for bacterial translocation in experimental cirrhosis. J Hepatol (2019), https://doi.org/10.1016/j.jhep.2019.06.017

[26] Gadaleta RM, van Erpecum KJ, Oldenburg B, et al. Farnesoid X receptor activation inhibits inflammation and preserves the intestinal barrier in inflammatory bowel disease. Gut 2011;60:463–472.
[27] Massafra V, Ijssennagger N, Plantinga M, et al. Splenic dendritic cell involvement in FXR-mediated amelioration of DSS colitis. BBA 2016;1862:166–173.
[28] Jia W, Xie G, Jia W. Bile acid-microbiota crosstalk in gastrointestinal inflammation and carcinogenesis. Nat Rev Gastroenterol Hepatol 2017.
[29] Renga B, D'Amore C, Cipriani S, et al. FXR mediates a chromatin looping in the GR promoter thus promoting the resolution of colitis in rodents. Pharmacol Res 2013;77:1–10.
[30] Inagaki T, Moschetta A, Lee YK, et al. Regulation of antibacterial defense in the small intestine by the nuclear bile acid receptor. PNAS 2006;103:3920–3925.
[31] Jakobsson HE, Rodriguez-Pineiro AM, Schutte A, et al. The composition of the gut microbiota shapes the colon mucus barrier. EMBO Rep 2015;16:164–177.
[32] Stappenbeck TS, Hooper LV, Gordon JI. Developmental regulation of intestinal angiogenesis by indigenous microbes via Paneth cells. PNAS 2002;99:15451–15455.
[33] Abraldes JG, Pasarin M, Garcia-Pagan JC. Animal models of portal hypertension. World J Gastroenterol 2006;12:6577–6584.
[34] Domenicali M, Caraceni P, Giannone F, et al. A novel model of CCl4-induced cirrhosis with ascites in the mouse. J Hepatol 2009;51:991–999.
[35] Ionac M. One technique, two approaches, and results: thoracic duct cannulation in small laboratory animals. Microsurgery 2003;23:239–245.
[36] Downes M, Verdecia MA, Roecker AJ, et al. A chemical, genetic, and structural analysis of the nuclear bile acid receptor FXR. Mol Cell 2003;11:1079–1092.
[37] Pellicciari R, Fiorucci S, Camaioni E, et al. 6alpha-ethyl-chenodeoxycholic acid (6-ECDCA), a potent and selective FXR agonist endowed with anticholestatic activity. J Med Chem 2002;45:3569–3572.
[38] Fang S, Suh JM, Reilly SM, et al. Intestinal FXR agonism promotes adipose tissue browning and reduces obesity and insulin resistance. Nat Med 2015;21:159–165.
[39] Roda A, Aldini R, Camborata C, et al. Metabolic profile of obeticholic acid and endogenous bile acids in rats with decompensated liver cirrhosis. Clin Transl Sci 2017;10:292–301.
[40] Brugiroux S, Beutler M, Pfann C, et al. Genome-guided design of a defined mouse microbiota that confers colonization resistance against Salmonella enterica serovar Typhimurium. Nat Microbiol 2016;2:16215.
[41] Wiest R, Cadelina G, Milstien S, McCuskey RS, Garcia-Tsao G, Groszmann RJ. Bacterial translocation up-regulates GTP-cyclohydrolase I in mesenteric vasculature of cirrhotic rats. Hepatology 2003;38:1508–1515.
[42] Fouts DE, Torralba M, Nelson KE, Brenner DA, Schnabl B. Bacterial translocation and changes in the intestinal microbiome in mouse models of liver disease. J Hepatol 2012;56:1283–1292.
[43] Verbeke L, Farre R, Verbinnen B, et al. The FXR agonist obeticholic acid prevents gut barrier dysfunction and bacterial translocation in cholestatic rats. Am J Pathol 2015;185:409–419.
[44] Gustot T, Fernández J, Szabo G, et al. Sepsis in alcohol-related liver disease. J Hepatol 2017;67:1031–1050.
[45] Pelaseyed T, Bergstrom JH, Gustafsson JK, et al. The mucus and mucins of the goblet cells and enterocytes provide the first defense line of the gastrointestinal tract and interact with the immune system. Immunol Rev 2014;260:8–20.
[46] Bergstrom KS, Kissoon-Singh V, Gibson DL, et al. Muc2 protects against lethal infectious colitis by disassociating pathogenic and commensal bacteria from the colonic mucosa. PLoS Pathog 2010;6 e1000902.
[47] Van der Sluis M, De Koning BA, De Bruijn AC, et al. Muc2-deficient mice spontaneously develop colitis, indicating that MUC2 is critical for colonic protection. Gastroenterology 2006;131:117–129.
[48] Sodhi CP, Neal MD, Siggers R, et al. Intestinal epithelial Toll-like receptor 4 regulates goblet cell development and is required for necrotizing enterocolitis in mice. Gastroenterology 2012;143:708–718.e705.
[49] Kandori H, Hirayama K, Takeda M, Doi K. Histochemical, lectin-histochemical and morphometrical characteristics of intestinal goblet cells of germfree and conventional mice. Exp Anim 1996;45:155–160.
[50] Schutte A, Ermund A, Becker-Pauly C, et al. Microbial-induced meprin beta cleavage in MUC2 mucin and a functional CFTR channel are required to release anchored small intestinal mucus. PNAS 2014;111:12396–12401.
[51] Stykova E, Nemcova R, Valocky I, Novotny F, Guba P. Adherence of bacteria to mucus collected from different parts of the reproductive tract of heifers and cows. Can J Microbiol 2013;59:720–725.
[52] Corfield AP, Wagner SA, Clamp JR, Kriaris MS, Hoskins LC. Mucin degradation in the human colon: production of sialidase, sialate O-acetylesterase, N-acetylneuraminate lyase, arylesterase, and glycosulfatase activities by strains of fecal bacteria. Infect Immun 1992;60:3971–3978.
[53] Llorente C, Jepsen P, Inamine T, et al. Gastric acid suppression promotes alcoholic liver disease by inducing overgrowth of intestinal Enterococcus. Nat Commun 2017;8:837.
[54] Hartmann P, Chen P, Wang HJ, et al. Deficiency of intestinal mucin-2 ameliorates experimental alcoholic liver disease in mice. Hepatology 2013;58:108–119.
[55] Uchimura Y, Fuhrer T, Li H, et al. Antibodies set boundaries limiting microbial metabolite penetration and the resultant mammalian host response. Immunity 2018;49:545–559.e545.
[56] Liebner S, Corada M, Bangsow T, et al. Wnt/beta-catenin signaling controls development of the blood-brain barrier. J Cell Biol 2008;183:409–417.
[57] Juliette Mouries IS, Edina Hot, Alessandra Silvestri, Marcel Sorribas Olivera, Erika Mileti, Reiner Weist, Luciano Adorini, Giuseppe Penna and Maria Rescigno. Microbiota-dependent gut vascular barrier disruption is required for NASH development: protective role of FXR activation by obeticholic acid; Journal of Hepatology. 2018;revision after 1st submission pending.
[58] Strickland LA, Jubb AM, Hongo JA, et al. Plasmalemmal vesicle-associated protein (PLVAP) is expressed by tumour endothelium and is upregulated by vascular endothelial growth factor-A (VEGF). J Pathol 2005;206:466–475.
[59] Wisniewska-Kruk J, van der Wijk AE, van Veen HA, et al. Plasmalemma vesicle-associated protein has a key role in blood-retinal barrier loss. Am J Pathol 2016;186:1044–1054.
[60] Schwabl P, Hambruch E, Seeland BA, et al. The FXR agonist PX20606 ameliorates portal hypertension by targeting vascular remodelling and sinusoidal dysfunction. J Hepatol 2016.
[61] Verbeke L, Farre R, Trebicka J, et al. Obeticholic acid, a farnesoid X receptor agonist, improves portal hypertension by two distinct pathways in cirrhotic rats. Hepatology 2014;59:2286–2298.
[62] Modica S, Petruzzelli M, Bellafante E, et al. Selective activation of nuclear bile acid receptor FXR in the intestine protects mice against cholestasis. Gastroenterology 2012;142, 355-365.e351-354.
[63] Jia W, Xie G, Jia W. Bile acid-microbiota crosstalk in gastrointestinal inflammation and carcinogenesis. Nat Rev Gastroenterol Hepatol 2018;15:111–128.
[64] Renga B, Cipriani S, Carino A, Simonetti M, Zampella A, Fiorucci S. Reversal of endothelial dysfunction by GPBAR1 agonism in portal hypertension involves a AKT/FOXOA1 dependent regulation of H2S generation and endothelin-1. PLoS ONE 2015;10 e0141082.
[65] He F, Li J, Mu Y, et al. Downregulation of endothelin-1 by farnesoid X receptor in vascular endothelial cells. Circ Res 2006;98:192–199.

Please cite this article in press as: Sorribas M et al. FXR-modulates the gut-vascular barrier by regulating the entry sites for bacterial translocation in experimental cirrhosis. J Hepatol (2019), https://doi.org/10.1016/j.jhep.2019.06.017